MAX-PLANCK INSTITUTE FOR POLYMER RESEARCH

JOHANNES GUTENBERG UNIVERSITY MAINZ

DISSERTATION

Electrical Degradation of Polymer Light-Emitting Diodes

Quan Niu

Dekan:

1. Gutachter:

2. Gutachter:

Tag der mündlichen Prüfung:

Affidavit

I hereby confirm that I have completed the present dissertation independently and without inadmissible external support. I have not used any sources or tools other than those indicated and have identified literal and analogous quotations.

Furthermore, I confirm that this thesis has not yet been submitted as part of another examination process neither in identical nor in similar form.

Place, date:

Signature:

Table of Contents

Scope of this thesis

Since Tang and VanSlyke reported the world's first efficient organic thin film light-emitting diodes based on thermally evaporated small molecules (OLEDs) in 1987,[1] followed by the discovery of the first solution-processed polymer based LED (PLED) in 1990 by Friend et al., [2] organic light-emitting diodes have attracted a lot of attention in the last 30 years. Organic light-emitting diodes based on emissive organic semiconductors, which include both polymers (PLED) and small molecules (OLED), have been viewed as a promising candidate to realize large-scale, ultrathin and flexible displays and lighting systems. Recently, OLEDs based on evaporated small molecules with optimized device architectures have already entered the display market, ranging from displays of smart phones to large TV screens. Furthermore, applications are foreseen in wearable electronics and the lighting market, where a number of prototypes have been demonstrated. However, one big challenge that limits a wider application of OLEDs and PLEDs is their device lifetime. Nowadays, efficient red and green OLEDs based on phosphorescence with sufficient lifetime for display applications have been developed. [3-6] However, phosphorescent blue emitters with an efficiency and lifetime comparable to those of red and green emitters have not been realized yet. For the commonly known blue phosphors, like iridium (III) bis[(4,6- difluorophenyl)-pyridinato-N,C′20] picolinate (FIrpic), a *LT50* lifetime (the time when the luminance drops to 50% of the initial value) at an initial luminance L_0 of 1000 cd/m^2 of only several hours has been reported, which is far away from application requirements.[7,8] Furthermore, for lighting applications that require high luminance, the lifetime of OLEDs still needs to be significantly improved.

Although a large effort has been put into understanding the mechanism of OLED degradation in the past decades, the 'intrinsic' degradation mechanism, which implies device efficiency loss under long-term electrical operation, is still under debate.

Thermally evaporated small molecule based OLEDs, as being used in today's display industry, have a complex device structure in order to realize high efficiency. The OLED structure consists of (doped) hole-injection, -transport and -blocking layers, (doped) electron-injection, -transport and -blocking layers, and an emissive layer, which consists of two or more materials. These materials serve as host matrix and guest emitter, respectively. The multi-layer structure and many-material system strongly complicates the disentanglement of mechanisms that lead to device fatigue.

Solution processed polymer-based LEDs are attractive because of their ease of processing, which allows cheap production via printing technology. However, typical PLEDs have an *LT50* lifetime of (a few) thousand hours at 1000 cd/m^2. For market introduction of PLEDs their lifetime needs to be significantly improved. However, for spin-coated PLEDs, even though they have a simple single-layer structure, the degradation mechanisms are also not well understood yet. In this thesis, the mechanisms of PLED degradation are discussed in Chapter 2 and 3. In Chapter 2, based on the recently developed understanding of PLED operation, numerical modelling is applied to device characteristics of pristine and degraded PLEDs. Possible mechanisms, including increase of the charge injection barrier, decrease of charge carrier mobility and increase of electron traps, are disentangled. It is found that the formation of hole traps is the only process that can explain the electrical characteristics of PLEDs upon degradation. By means of transient electroluminescence measurements, the decrease of the hole transport is experimentally verified.

Subsequently in Chapter 3, by analyzing the voltage drift with a numerical device model, the amount of hole traps as a function of aging time under PLED stress is derived. It is found the hole trap concentration increases with the square-root of time after an initial short aging period and is linearly proportional to the current density. The dependence of the voltage drift on PLED thickness is also consistently explained. With the amount of hole traps known the light-output of the PLED is well predicted as

a function of aging time. The observed trap formation rate points to exciton-polaron interaction as the mechanism behind PLED degradation.

In Chapter 4, the information of hole trap formation during PLED degradation is used to understand the origin of negative differential capacitance (NC) observed at low frequencies in PLEDs. We systematically vary the amount of electron and hole traps in the polymeric semiconductor. Increasing the electron and hole trap density enhances the NC effect. The magnitude and observed decrease of the relaxation time is consistent with the (inverse) rate of trap-assisted recombination. The absence of NC in a nearly trap-free PLED unambiguously shows that trap-assisted recombination is the responsible mechanism for the negative contribution to the capacitance in bipolar organic diodes.

In Chapter 5, the degradation of blue phosphorescent small molecule light-emitting diode (PHOLED) is investigated. In order to disentangle the contribution of the electrons and holes on the transport and efficiency of both pristine and degraded PHOLEDs transient electroluminescence measurements[9] are applied. By varying the concentration of hole transporting units it is shown the electron transport is dominant for pristine PHOLEDs. Furthermore, degradation of the PHOLEDs upon electrical aging is not related to the hole transport, but is governed by a decrease of the electron transport due to the formation of electron traps.

Reference

[1] C. W. Tang, S. A. VanSlyke. *Applied physics letters* **1987**, *51*, 913.

[2] J. Burroughes, D. Bradley, A. Brown, R. Marks, K. Mackay, R. Friend, P. Burns, A. Holmes. *nature* **1990**, *347*, 539.

[3] S. H. Kim, J. Jang, J. Y. Lee. *Applied physics letters* **2007**, *90*, 203511.

[4] B. D. Chin, C. Lee. *Advanced Materials* **2007**, *19*, 2061.

[5] A. B. Chwang, R. C. Kwong, J. J. Brown. *Applied physics letters* **2002**, *80*, 725.

[6] R. C. Kwong, M. R. Nugent, L. Michalski, T. Ngo, K. Rajan, Y.-J. Tung, M. S. Weaver, T. X. Zhou, M. Hack, M. E. Thompson. *Applied Physics Letters* **2002**, *81*, 162.

[7] R. Holmes, S. Forrest, Y.-J. Tung, R. Kwong, J. Brown, S. Garon, M. Thompson. *Applied physics letters* **2003**, *82*, 2422.

[8] R. Seifert, I. R. de Moraes, S. Scholz, M. C. Gather, B. Lüssem, K. Leo. *Organic Electronics* **2013**, *14*, 115.

[9] P. W. M. Blom, M. C. J. M. Vissenberg. *Physical Review Letters* **1998**, *80*, 3819.

Chapter 1 Introduction

In this chapter, the chemical structures and charge transport properties of organic semiconductors are discussed. To understand the operation of single-layer polymer based light emitting diodes (PLEDs), the device characteristics, including electron and hole current and the recombination processes, are introduced. Finally, an overview of previous research on the degradation of OLEDs and PLEDs is presented.

1.1 Organic semiconductors

Electric conductivity in organic materials was early discussed in the 1950s. At that moment, the main focus was on organic small molecules with a crystalline structure, such as anthracene and naphthalene.[1,2] However, the electric conductivity in these organics is very low, which makes them behave like insulators. They were cataloged as semiconductors since they exhibit semiconducting properties such as photo-conductivity and electroluminescence.[3] High electric conductivity of organics was first reported in chemically doped polyacetylene in 1977. [4] Since the 1980s, two breakthroughs, being world's first efficient thin film OLED based on organic small molecules, and later on the first polymer based LED, [5,6] have triggered intensive research on undoped organic semiconductors and corresponding electric devices.

The chemical structures of organic semiconductors, either polymers or small molecules, are characterized by conjugated π-bonds, which are responsible for their semiconducting properties. Conjugation means alternating single and double bonds. For example, in the chemical structures of a benzene molecule (Figure 1), six carbon atoms are connected with each other via covalent σ-bond, resulting from the overlap

of two hybrid sp^2 orbitals of carbon atoms. Another orbital, which is perpendicular to the sp^2 hybridization plane, is the p_z orbital. For adjacent carbon atoms the p_z orbital overlap to form conjugated π bonds. Within these bonds electrons are free to move from one atom to another, called delocalization. The unfilled anti-bonding orbital of the π-bond corresponds to the lowest unoccupied molecular orbital (LUMO) of the molecule, and the filled bonding orbital corresponds to the highest occupied molecular orbital (HOMO).

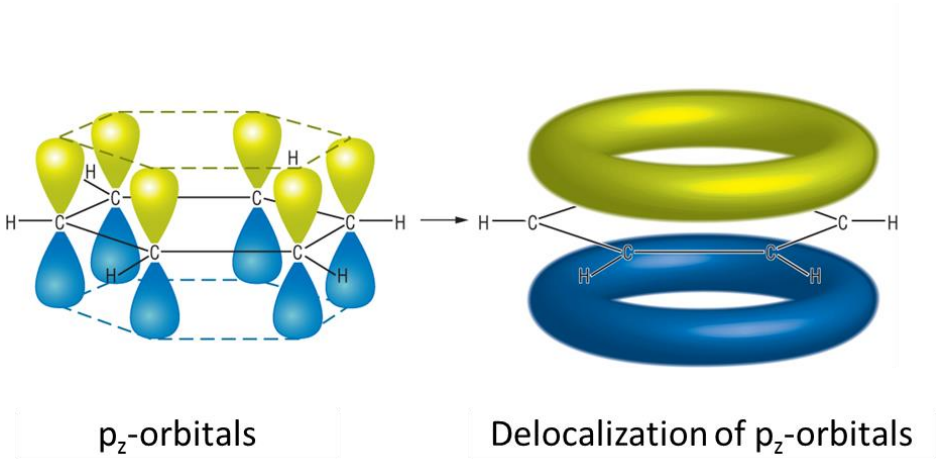

Figure 1. Scheme of conjugation in the chemical structure of a benzene molecule.

1.2 Charge transport in Organic semiconductors

Although the conjugated π-bond can provide a delocalization of electrons, the weak intermolecular interactions via van der Waals or London forces prevent strong orbital overlap between molecules and delocalization in a long range. In case of a conjugated polymer, the kinks and defect in the polymer chains can also break the conjugation, and therefore the delocalization. Compared to their inorganic counterparts, where atoms are strongly bound by covalent- or ionic bonds, allowing charges to be easily transported, the charge transport in organic material semiconductors is rather difficult. In 1956, Conwell and Mott proposed a new model for charge transport between the

impurity sites in inorganic semiconductors. [7] At low concentrations, the impurity states, with energy levels inside the semiconductor bandgap, cannot form a 'conducting band' due to the weak atomic/molecular interactions due to the large separation distance. In this case, carriers need to overcome the energy barrier between two localized states by tunneling/ 'hopping' with the assistance of phonons. The transition rate for a carrier to 'hop' from one occupied site i with energy ξ_i to another unoccupied site j with energy ξ_j with a phonon frequency v_0 was proposed by Miller and Abrahams: [8]

$$\nu_{i\to j} = \nu_0 \exp(-2\gamma a \frac{R_{ij}}{a}) \begin{cases} \exp\left[-\left(\xi_i - \xi_j\right)/k_B T\right] for \xi_i > \xi_j, \\ 1 for \xi_i < \xi_j \end{cases} \quad (1)$$

Where γ is the inverse localization length, R_{ij} is the distance between the states i and j, a is the average lattice distance and k_B is the Boltzmann constant. The first exponential term from equation [1] represents the tunneling probability determined by the orbital overlap of state i and j, and the second exponential term accounts for the temperature dependence of the phonon density.

In organic semiconductors, charge transport is realized by carriers to 'hop' from one conjugated site to another. In early studies, time-of-flight measurements were applied to investigate the charge transport properties of organic semiconductors. It was found that for many disordered organic semiconductors the charge-carrier mobility is thermally activated at low electric fields, and follows a Poole-Frenkel like dependence at high field. This feature was described by an empirical law, given by

$$\mu_p(E) = \mu_0 \exp\left[-\frac{\Delta}{k_B T} + B(\frac{1}{k_B T} - \frac{1}{k_B T_0})\sqrt{E}\right] \quad (2)$$

with μ_0 the zero-field mobility, Δ the zero-field activation energy, and E the applied electrical field. In 1993, Bässler published a review on the charge transport properties

of a disordered organic solid by Monte Carlo simulations.[9] By using a density of states that is Gaussianly distributed in energy, and Miller-Abrahams hopping rates, it was found that the simulated temperature- and field dependence of the mobility μ_{GDM} (Gaussian Disorder Model) could be approximated by the analytical expression:

$$\mu_{GDM} = \mu_{\infty} \exp\left[-\left(\frac{2\sigma}{3k_B T}\right)^2\right] \times \begin{cases} \exp\left[C\left(\left(\frac{\sigma}{k_B T}\right)^2 - \Sigma^2\right)\sqrt{E}\right] & for \Sigma \geq 1.5 \\ \exp\left[C\left(\left(\frac{\sigma}{k_B T}\right)^2 - 2.25\right)\sqrt{E}\right] & for \Sigma < 1.5 \end{cases} \quad (3)$$

where μ_{∞} is the mobility in the limit $T \rightarrow \infty$, with typical values between 10^{-6} and 10^{-5} m^2/Vs, , σ is the width of the Gaussian density of states, C is a constant that depends on the site spacing, and Σ is the degree of positional disorder.

It should be noted that Bässler's simulations are based on one-particle transport, which ignores the influence of a finite carrier density. In 1998, Vissenberg and Matters developed a model to describe the charge transport in organic field-effect transistors by taking into account the filling of localized states by injected charges.[10] Later on, Tanase et al. experimentally verified the charge density dependence of the mobility in organic semiconductors.[11] It was explained that the mobility of a single polymeric semiconductor can vary orders of magnitude when measured in either a diode or a transistor. The reason is that the charge density in a transistor is three orders of magnitude larger as compared to the density in a diode. The density dependence of mobility is especially dominant at room temperature and higher temperatures. For lower temperatures, the field-dependence of mobility becomes more and more pronounced.

By taking into account the density-, field- and temperature dependence of mobility and solving the master equation for hopping transport in Gaussianly distributed

energy sites, Pasveer et al.[12] provided an extended description for the charge carrier mobility μ_{EGDM} (Extended Gaussian Disorder Model) in organic semiconductors, given by:

$$\mu_{EGDM}(T, p, E) = \mu_p(T, p)\mu_E(T, E) \tag{4a}$$

where

$$\mu_p(T, p) = \mu_0 \exp\left(-0.42\left(\frac{\sigma}{k_B T} \right)^2 + \frac{1}{2}\left(\left(\frac{\sigma}{k_B T} \right)^2 - \frac{\sigma}{k_B T} \right)\left(2pa^3\right)^{\delta} \right) \tag{4b}$$

and

$$\mu_E(T, E) = \exp\left(0.44\left(\left(\frac{\sigma}{k_B T} \right)^{3/2} - 2.2 \right)\sqrt{1 + 0.8\left(\frac{Eea}{\sigma} \right)^2 - 1} \right) \tag{4c}$$

The exponent δ in (4b) is given by

$$\delta = 2\frac{\ln\left(\left(\sigma k_B T\right)^2 - \sigma / k_B T\right) - \ln\left(\ln 4\right)}{\left(\sigma / k_B T\right)^2} \tag{5}$$

It was demonstrated that the combination of space-charge limited current and μ_{EGDM} provided a consistent description of the hole transport in various poly(p-phenylene vinylene) (PPV) derivatives.

1.3 Operation of a polymer light emitting diode

In the simplest structure of a PLED, one layer of conjugated polymer is sandwiched between two electrodes. When a bias is applied both electrons and holes are injected into the semiconducting layer. Due to the applied electric field electrons and holes will travel to the opposite electrode. When the distance between a hole and an electron is such that their Coulomb binding energy exceeds *kT*, they will form an excited state, called exciton. The exciton subsequently decays to its ground state by the emission of a photon. . The operation of a PLED is then determined by three processes: charge

injection, hole- and electron transport and recombination. For efficient injection, Ohmic contacts are preferred for both electrons and holes. . Therefore, cathode and anode materials are chosen such that their work functions align with the LUMO and HOMO of the organic semiconductor, respectively. Due to the difference between the work functions of the anode and cathode an internal field is built-up. This built-in voltage first needs to be overcome by the applied voltage before efficient charge injection takes place.

In next sections, the electron- and hole transport and their recombination will be discussed.

1.4 Hole- and electron transport in a PLED

To investigate the hole transport and electron transport in a PLED separately, contact materials can be chosen in such a way that only unipolar transport takes place. For example, in a hole-only device based on Poly(p-phenylene vinylene) (PPV) derivatives, high work function materials such as PEDOT:PSS, Au or Mo_2O_3 are utilized. At the positively biased anode the high work function electrode forms an Ohmic contact for efficient hole injection. . At the negatively biased electrode (cathode) the high work function electrode gives rise to a large electron injection barrier, such that electron injection into the device is blocked. A device with two high work function electrodes is called a hole-only device. Similarly, a device with two low work function electrodes, where hole injection is blocked is termed an electron-only device. The schematic structures of a PPV-based hole-only device and an electron-only device are shown in Figure 2.

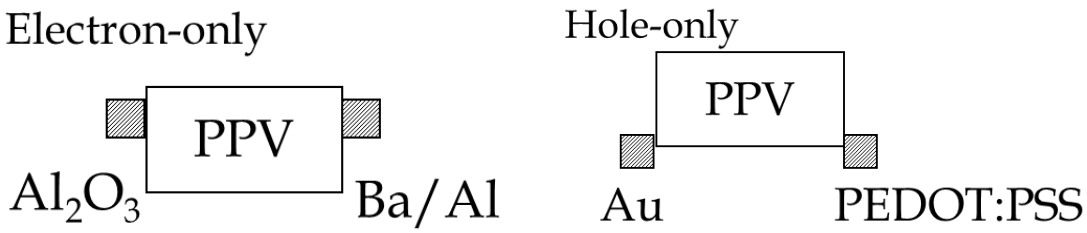

Figure 2. Energy level scheme of PPV based electron-only and hole-only devices.

Due to the low concentration of intrinsic charges in undoped organic semiconductors, charges injected by the electrodes due to an applied voltage V are not compensated. Instead, space-charges are formed across the semiconducting layer, such that further injection of carriers is electrostatically limited. The corresponding space-charge limited current (SCLC) is described by the Mott-Gurney law: [13]

$$J = \frac{9}{8}\varepsilon_0\varepsilon_r\mu\frac{V^2}{L^3} \qquad (6)$$

with ε_0 is the permittivity of vacuum, ε_r is the relative dielectric constant of the semiconductor, μ is the carrier mobility and L the thickness of the device. Already in 1996 it was demonstrated that the hole current in PPV-based diodes obeyed the Mott-Gurney law at low electric fields.

In contrast, in electron-only devices the electron current is found to deviate from the Mott-Gurney law. Here, a steeper voltage- and thickness dependence was observed (ref). Furthermore, compared to the SCL hole current, the electron current in PPV-derivatives is orders of magnitude lower. These characteristics are generally explained by the presence of electron traps in the band gap that limit the electron current. The influence of traps on a space-charge limited current was first discussed in 1956 by Lampert for a single trap level.[14] In 1962, Mark and Helfrich (MH) provided a description for the trap-limited current in a semiconductor where the traps are distributed in energy in the bandgap. [15] Assuming an exponential distribution of trap states inside the semiconductor bandgap, given by

$$n_t(E) = \left(\frac{N_t}{k_B T_t}\right) \exp\left(\frac{\xi - \xi_c}{k_B T_t}\right) \qquad (7)$$

with $n_t(\xi)$ the trap density of states at energy ξ, ξ_c the energy of the conduction band, N_t the total density of traps, and $k_B T_t$ an energy characterizing the trap distribution. The trap-limited current is then given by

$$J = N_c e \mu_n \left(\frac{\varepsilon_0 \varepsilon_r}{e N_t}\right)^r \frac{V^{r+1}}{L^{2r+1}} C(r) \qquad (8)$$

with μ_n the electron mobility, $r=T_t/T$, N_c the effective density of states in the conduction band, and $C(r)=r^r(2r+1)^{r+1}(r+1)^{-2r-1}$.

Although the MH model consistently described the electron current of a PPV-derivative at room temperature it failed to describe the temperature dependence of the trap-limited electron currents. In 2007, Mandoc et al. modified the MH formulism by taking into account the Gaussianly distributed density of states (DOS) of the LUMO.[16] Furthermore, for the free electrons a density-, field- and temperature dependent mobility was used. With that modification the current of PPV-based electron-only devices was consistently described. Later on, it was demonstrated by Nicolai et al. that the electron currents in PPV could also be described by a model based on Gaussianly distributed trap states.[17] It was argued that, since the localized states in the HOMO and LUMO exhibit a Gaussian distribution due to disorder, also trap states are broadened by disorder resulting in a Gaussian distribution. The occupation of the trap states is then calculated by solving the integral of the product of the Gaussian DOS with the Fermi-Dirac function using an approximation introduced by Paasch and Scheinert.[18] Implementing this approximation into a numerical model, which further takes into account the diffusion of carriers, a density-, field- and temperature dependent mobility, the *J-V* characteristics of electron-only devices based

on various PPV derivatives can be consistently modeled Applying the model based Gaussianly distributed electron traps to a whole range of semiconducting polymers it was found that the electron traps for all these polymers are identical.[19] The trap energy level is centered at 3.6 eV below vacuum, the trap density amounts to ~3×10^{23} m^{-3} with a typical distribution width of 0.1 eV. This suggests that the electron traps in a large range of conjugated polymers originate from the same species. A possible candidate could be hydrated oxygen complexes, with an energy level of 3.7 eV below vacuum for the $(H_2O)_2$-O_2 complex.[19]

1.5 Recombination in polymer light-emitting diodes

Another very important process in PLEDs, which determines their efficiency, is the recombination of free holes and free electrons. The rate (R_L) of this bi-molecular recombination is proportional to the product of density of free holes (p) and density of free electrons (n) with a rate constant B_L: [20]

$$R_L = B_L(np - n_1 p_1) \qquad (9)$$

where n_1 and p_1 are intrinsic concentrations of electrons and holes at thermal equilibrium. In 1995, with Mont Carlo simulations Bässler et al. suggested that the bi-molecular recombination in organic semiconductors with hopping transport is of the Langevin-type.[21] In Langevin recombination, he recombination rate is determined by the diffusion of free charges towards each other within their mutual Coulomb field. Here, the rate constant amounts to

$$B_L = \frac{e}{\varepsilon_0 \varepsilon_r}(\mu_n + \mu_p) \qquad (10)$$

with e the elementary charge, and μ_n and μ_p the electron and hole mobility (which

depend on the temperature, electric field and charge density)respectively. Langevin recombination is typical for materials where the charge carrier mean free path is smaller than a critical Coulombic capture radius $r_c = e^2/4\pi\varepsilon_o\varepsilon_r kT$. In the organic semiconductors the mean free path, i.e. the hopping distance of charge carriers, is around 1-3 nm. At room temperature, the critical capture radius is around 18.5 nm, which supports the occurrence of Langevin recombination in organic semiconductors.[22] In 1997, Blom et al. verified the occurrence of Langevin recombination in polymer LEDs experimentally.[23] By modelling the temperature dependence of the *J-V* characteristics of hole-only and double carrier PLEDs it was found that the bi-molecular recombination constant B_L is thermally activated. The activation energy was identical to the free charge carrier mobility, as predicted by equation [10].

However, comparing the experimentally obtained bi-molecular recombination constant with the value calculated from equation [10] a small discrepancy was observed. As a possible explanation for this discrepancy the occurrence of trap-assisted recombination was proposed. This type of recombination, which is the dominant recombination process in silicon, was first described by Shockley, Read and Hall in 1952. [24]The SRH recombination is schematically indicated in Figure 3. First, an electron is captured by an empty orbital within the bandgap (3b) with a rate determined by the capture coefficient C_n The trapped electron can either be thermally excited back to conduction band (3c) or is being captured by a free hole (3d) with a capture coefficient C_p;

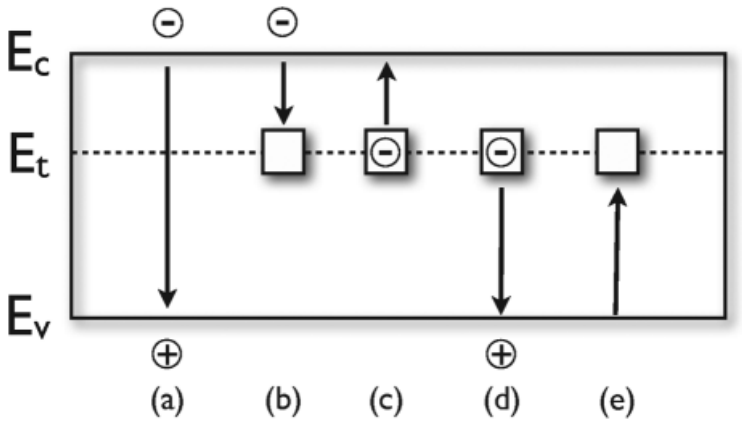

Figure 3. Schematic representation of bimolecular recombination and four processes involved in trap-assisted recombination: (a) bimolecular recombination, (b) electron capture, (c) electron emission, (d) hole capture, (e) hole emission. [24]

Assuming thermal equilibrium between these four processes, the rate of trap-assisted recombination, also named Shockley-Read-Hall (SRH) recombination, is given by

$$R_{SRH} = B_{SRH}(np - n_1 p_1) \qquad (11)$$

with:

$$B_{SRH} = C_n C_p N_t / \left[C_n (n + n_1) + C_p (p + p_1) \right] \qquad (12)$$

The electron capture coefficient C_n donates the probability for the electrons in the conduction band to be captured by the empty trap orbitals per unit time. C_p is the probability of a free hole to be captured by a trapped electron. Due to momentum conservation the process is accompanied by the release of a phonon. Experimentally, by investigating the open-circuit voltage dependence of a PPV-based PLED as a function of light intensity, the SRH recombination rate was measured.[25] It was found that SRH recombination in organic semiconductors is dominated by the diffusion of free carriers towards the trapped charges within their mutual Coulomb field. [25] In case of electron traps, the SRH recombination rate and the capture coefficient for trapped electrons to capture free holes can be approximated by : [22]

$$R_{SRH} = C_p N_t p \quad (13)$$

and:

$$C_p = \frac{q}{\varepsilon}\mu_p \quad (14)$$

As a consequence, once the charge-carrier mobility and trapping parameters for holes and electrons are known, the recombination processes, including Langevin and SRH recombination, and efficiency of PLEDs can be predicted.[22]

1.6 Electrical degradation of PLEDs and OLEDs

To test the stability of PLEDs and OLEDs typically a constant current is applied to stress the devices. Typically, the degradation of PLEDs and OLEDs is characterized by an increase of the driving voltage and a decrease of the light-output with increasing aging time.

For PLEDs based on solution-processed fluorescent polymers, the device structure is simple with one layer of emissive polymer sandwiched between two electrodes. From early work of Parker et al. it was found that hole-only devices based on poly(2-methoxy-5-(3′,7′-dimethyloctyloxy))-1,4-phenylene vinylene (MDMO-PPV) do not degrade upon long-term electrical stress, whereas double carrier PLEDs exhibit a voltage increase and luminance decrease.[26] Based on this observation it was concluded that the electron transport causes the degradation of PLEDs. As a possible origin for degradation, it was proposed that the electron mobility will decrease during degradation due to the formation of electron traps.[26] Such traps could be aromatic aldehydes or esters arising from oxidation of vinyl bonds in the polymer backbone. A decrease of the electron transport upon stress was also reported for PPV-based planar electro-chemical cells, indicated by a shift of the recombination zone towards the

cathode.[27]

Furthermore, by varying the current density as well as comparing degradation of MDMO-PPV LEDs in AC and DC mode, it was found that the voltage increase was proportional to the total amount of charge that passed through the devices.[26] Silvestre et al. demonstrated that the voltage drift and light degradation of PLEDs are related.[28] They proposed that non-radiative recombination with higher energy that does not contribute to the light-output is responsible for the formation of deep traps. These deep traps then lead to an increase of low energy transitions that slow down the degradation. For the rate of trap formation an empirical relation was used with parameters of which the physical meaning is not fully clear. Furthermore, it was not specified whether the deep traps are electron- or hole traps and also the rate of trap formation was not quantitatively addressed. In recent work by Stegmaier et al. a decrease of the hole transport during PLED aging was demonstrated by using time of flight measurement.[29] It was found that the combination of electrical and optical stress leads to a decreased hole transport, most probably caused by the formation of hole traps.

In a recent review by Gassmann et al.[30] the impact of chemical impurities as halogen defects, which might affect the cathode or act as electron trap, molecular weight and chemical structure on the PLED lifetime were addressed. It was also reported that the amount of triplet state excitons, which have a relatively long lifetime, negatively affect the lifetime of a PLED. Triplet excitons recombine non-radiatively and therefore produce heat. Furthermore, they might activate triplet oxygen to singlet oxygen, which will subsequently attack the vinyl bonds of PPV. As a possible mechanism for the decrease of the hole transport in the presence of electrons the formation of deep hole traps was suggested, which is known to lead to longer transit times in time of flight (TOF) measurements.[31] Furthermore, the *J-V* characteristics of a degraded PLED were modelled by assuming a decrease of the hole mobility, while keeping μ_p/μ_n (ratio between hole mobility and electron mobility) constant. For electrons, a single trap level was assumed that was kept constant during degradation.[30] However, the non-radiative recombination between free holes and

trapped electrons, which is an important loss process, was not taken into account. Summarizing, possible causes proposed for degradation were a decrease of charge carrier mobility, a reduced charge injection by the electrodes, or the formation of charge traps.

For the state-of-the art thermal evaporated small molecular OLEDs, which have recently been widely applied in display industry, investigation of the degradation mechanism is complicated by the multi-layer structure and in many cases guest-host emitting systems. Scholz et al. have reviewed the chemical degradation of iridium complex based phosphorescent materials, with emission colors covering the entire range of the visible spectrum.[32] By using laser desorption ionization time-of-flight mass spectrometry (LDI-TOF-MS), dissociation of such materials due to excitation processes is promoted. The dissociation product can then form stable complexes with adjacent materials e.g. hole blocking materials, which makes the reaction path irreversible.[33-35] Using hole blocking materials that do not show complex formation with emitters, highly stable devices can be obtained.[32,36] Next to the stability of the emitter also chemical degradation of host, electron transport and hole transport materials have been discussed.[37-41] Giebink et al. investigated the degradation of a blue PHOLED by modelling the dependence of luminance and voltage on aging time.[42] The aging behavior could be explained by assuming that hole traps will be formed under device fatigue. It was argued that generation of these defect sites originates from exciton-polaron interactions.[42] As a result, in many state-of-art device architectures, the transport of electrons and holes is separated by using host-guest emissive layers. [43-48] In such a composite layer the electron transport is for example governed by the emitting molecules, whereas the hole transport is carried by the host or by co-evaporated hole transport molecules. Such a design lowers the density of polarons on the emitter and significantly increases device lifetime.[43-49]
Another approach to disentangle various degradation mechanisms is by studying the effect of electrical stress on unipolar devices. For OLEDs with an emitting layer consisting of only one material, the fluorescent deep-blue emitter

spiro-4,40-Bis(2,2-diphenylvinyl)-1,10-biphenyl (Spiro-DPVBi), the stability of unipolar devices under a high current density of 100 mA/cm2 was traced.[50] Since unipolar devices showed an unchanged photoluminescence fluorescence intensity under electrical stress, whereas bipolar devices exhibited a sharp decline of both electroluminescence and photoluminescence efficiency, it was concluded that the device degradation is induced by excitons.[50] For aluminium-tris(8-hydroxychinolin) (Alq_3) -based OLEDs using a similar approach it was concluded that hole transport is the reason for the device degradation.[51] However, even in these relatively simple OLED structures extrapolation of the results of unipolar devices towards OLEDs is not straightforward, since in unipolar devices recombination processes are absent. As a result, the role played by excitons, as for example in exciton-polaron interactions, can be easily underestimated or overlooked.[51,52] For more complicated OLED structures consisting of various transport and blocking layers and host-guest emissive layers such extrapolation is even more complicated.

In the next chapters the degradation in a single layer PLED will be systematically investigated

Reference

[1] H. Mette, H. Pick. *Z. Physik* **1953**, *134*, 566.

[2] R. Kepler. *Physical Review* **1960**, *119*, 1226.

[3] K.-C. Kao, W. Hwang *Electrical transport in solids: with particular reference to organic semiconductors*; Oxford, 1979.

[4] C. K. Chiang, C. Fincher Jr, Y. W. Park, A. J. Heeger, H. Shirakawa, E. J. Louis, S. C. Gau, A. G. MacDiarmid. *Physical Review Letters* **1977**, *39*, 1098.

[5] C. W. Tang, S. A. VanSlyke. *Applied physics letters* **1987**, *51*, 913.

[6] J. Burroughes, D. Bradley, A. Brown, R. Marks, K. Mackay, R. Friend, P. Burns, A. Holmes. *nature* **1990**, *347*, 539.

[7] N. Mott. *Canadian journal of physics* **1956**, *34*, 1356.

[8] A. Miller, E. Abrahams. *Physical Review* **1960**, *120*, 745.

[9] H. Bässler. *phys. status solidi b* **1993**, *175*, 15.

[10] M. Vissenberg, M. Matters. *Physical Review B* **1998**, *57*, 12964.

[11] C. Tanase, P. W. M. Blom, D. M. de Leeuw. *Physical Review B* **2004**, *70*, 193202.

[12] W. Pasveer, J. Cottaar, C. Tanase, R. Coehoorn, P. Bobbert, P. Blom, D. De Leeuw, M. Michels. *Physical review letters* **2005**, *94*, 206601.

[13] N. F. Mott, R. W. Gurney. **1940**.

[14] M. A. Lampert. *Physical Review* **1956**, *103*, 1648.

[15] P. Mark, W. Helfrich. *Journal of Applied Physics* **1962**, *33*, 205.

[16] M. Mandoc, B. de Boer, G. Paasch, P. Blom. *Physical Review B* **2007**, *75*, 193202.

[17] H. Nicolai, M. Mandoc, P. Blom. *Physical Review B* **2011**, *83*, 195204.

[18] G. Paasch, S. Scheinert. *Journal of Applied Physics* **2010**, *107*, 104501.

[19] H. T. Nicolai, M. Kuik, G. Wetzelaer, B. De Boer, C. Campbell, C. Risko, J. Brédas, P. Blom. *Nature materials* **2012**, *11*, 882.

[20] P. Langevin. *Ann. Chim. Phys* **1903**, *28*, 443.

[21] U. Albrecht, H. Bässler. *physica status solidi (b)* **1995**, *191*, 455.

[22] M. Kuik, G. J. A. Wetzelaer, H. T. Nicolai, N. I. Craciun, D. M. De Leeuw, P. W. Blom, *Advanced Materials* **2014**, *26*, 512.

[23] P. Blom, M. De Jong, S. Breedijk. *Applied Physics Letters* **1997**, *71*, 930.

[24] W. Shockley, W. T. Read. *Physical Review* **1952**, *87*, 835.

[25] M. Kuik, L. Koster, G. Wetzelaer, P. Blom. *Physical review letters* **2011**, *107*, 256805.

[26] I. D. Parker, Y. Cao, C. Y. Yang. *Journal of Applied Physics* **1999**, *85*, 2441.

[27] J. Dane, J. Gao. *Applied Physics Letters* **2004**, *85*, 3905.

[28] G. C. M. Silvestre, M. T. Johnson, A. Giraldo, J. M. Shannon. *Applied Physics Letters* **2001**, *78*, 1619.

[29] K. Stegmaier, A. Fleissner, H. Janning, S. Yampolskii, C. Melzer, H. von Seggern. *Journal of Applied Physics* **2011**, *110*, 034507.

[30] A. Gassmann, S. V. Yampolskii, A. Klein, K. Albe, N. Vilbrandt, O. Pekkola, Y. A. Genenko, M. Rehahn, H. von Seggern. *Materials Science and Engineering: B* **2015**, *192*, 26.
[31] K. Stegmaier, A. Fleissner, H. Janning, S. Yampolskii, C. Melzer, H. v. Seggern. *Journal of Applied Physics* **2011**, *110*, 034507.
[32] S. Scholz, D. Kondakov, B. Lüssem, K. Leo. *Chemical Reviews* **2015**, *115*, 8449.
[33] S. Scholz, R. Meerheim, K. Walzer, K. Leo, *Photonics Europe* **2008**, 69991B.
[34] I. R. d. Moraes, S. Scholz, B. Lüssem, K. Leo. *Organic Electronics* **2011**, *12*, 341.
[35] M. J. Jurow, A. Bossi, P. I. Djurovich, M. E. Thompson. *Chemistry of Materials* **2014**, *26*, 6578.
[36] I. R. de Moraes, S. Scholz, B. Lüssem, K. Leo. *Organic Electronics* **2012**, *13*, 1900.
[37] D. Kondakov, W. Lenhart, W. Nichols. *Journal of Applied Physics* **2007**, *101*, 024512.
[38] D. Y. Kondakov, T. D. Pawlik, W. F. Nichols, W. C. Lenhart. *Journal of the Society for Information Display* **2008**, *16*, 37.
[39] D. Y. Kondakov. *Journal of Applied Physics* **2008**, *104*, 084520.
[40] S. Scholz, K. Walzer, K. Leo. *Advanced Functional Materials* **2008**, *18*, 2541.
[41] O. Molt, E. Fuchs, C. Lennartz, K. Kahle, N. Moonen, J. Rudolph, C. Schildknecht, G. Wagenblast, *Frontiers in Optics* **2007**, TWB3.
[42] N. C. Giebink, B. W. D'Andrade, M. S. Weaver, P. B. Mackenzie, J. J. Brown, M. E. Thompson, S. R. Forrest. *Journal of Applied Physics* **2008**, *103*, 044509.
[43] J. Shi, C. Tang. *Applied physics letters* **1997**, *70*, 1665.
[44] Y. Hamada, T. Sano, K. Shibata, K. Kuroki. *Japanese journal of applied physics* **1995**, *34*, L824.
[45] H. Kanno, Y. Hamada, H. Takahashi. *Selected Topics in Quantum Electronics, IEEE Journal of* **2004**, *10*, 30.
[46] J.-H. Lee, C.-I. Wu, S.-W. Liu, C.-A. Huang, Y. Chang. *Applied Physics Letters* **2005**, *86*, 103506.
[47] C. Eickhoff, P. Murer, T. Geßner, J. Birnstock, M. Kröger, Z. Choi, S. Watanabe, F. May, C. Lennartz, I. Stengel, *SPIE Organic Photonics+ Electronics* **2015**, 95662N.
[48] T. K. Hatwar, C. Brown, L. Cosimbescu, M. Ricks, J. P. Spindler, W. Begley, J. Vargas, *Optical Science and Technology, the SPIE 49th Annual Meeting* **2004**, 1.
[49] N. Giebink, B. D'Andrade, M. Weaver, J. Brown, S. Forrest. *Journal of Applied Physics* **2009**, *105*, 124514.
[50] S. Winter, S. Reineke, K. Walzer, K. Leo, **2008**, *6999*, 69992N.
[51] Z. D. Popovic, H. Aziz. *Selected Topics in Quantum Electronics, IEEE Journal of* **2002**, *8*, 362.
[52] Q. Wang, H. Aziz. *ACS applied materials & interfaces* **2013**, *5*, 8733.

Chapter 2 Modelling of electrical characteristics of degraded polymer light-emitting diodes

Degradation of a polymer light-emitting diode (PLED) driven under constant current is characterized by an increase of driving voltage and a decrease of luminance and efficiency. Possible causes for degradation can be a decrease of charge carrier mobility, a reduced charge injection by the electrodes, or the formation of charge traps. In order to disentangle these processes we have performed numerical simulations on the device characteristics of pristine and degraded PLEDs. The observed reduction in transport and luminous efficiency under current stress is simultaneously explained by the formation of hole traps. A reduction of the hole transport upon degradation was verified by transient electroluminescence measurements.

2.1 Introduction

As discussed in Chapter 1, possible causes proposed for PLED degradation were a decrease of charge carrier mobility, a reduced charge injection by the electrodes, or the formation of charge traps. As a first step to discriminate between these processes numerical simulations using a recently developed device model[1,2] were performed on the device characteristics of pristine and degraded PLEDs. In the simulations presented here, we first independently vary device parameters such as injection barrier, charge-carrier mobility, electron- and hole-traps, and study their effect on PLED performance. Experiments on super yellow PPV (SY-PPV) based PLEDs are used as a reference to compare with our simulation results. In this way we can exclude a number of processes, such as a decrease in mobility, the formation of electron traps by oxidation, and increased charge injection barriers as being responsible for the degradation of PLEDs. Our simulations show that the formation of hole traps during degradation is the only mechanism consistent with the observed voltage increase and decrease of light output and efficiency during stress. The decrease of PLED efficiency upon stress is a direct consequence of the additional non-radiative recombination of free electrons with trapped holes, which competes with the radiative Langevin recombination. Based on the simulations, the formation of hole traps also leads to a broadening of the emission zone. Consequently, the quenching of excitons at the cathode and anode plays a smaller role in degraded PLEDs. The formation of hole traps is further supported experimentally by hole transient time measurements for pristine and aged PLEDs using the transient electroluminescence method.[3]

2.2 PLED device model

To calculate the current density in a PLED, a numerical device model has been developed that includes electron trapping and a field- and density dependent free

carrier mobility.[1] The model is characterized by the current-flow equations:

$$J = J_n + J_p$$

$$J_n = e\mu_n[E(x), n(x)]n(x)E(x) + eD_n \frac{\partial}{\partial x} n(x) \quad (1)$$

$$J_p = e\mu_p[E(x), p(x)]p(x)E(x) - eD_p \frac{\partial}{\partial x} p(x)$$

the Poisson equation

$$\frac{\varepsilon_0 \varepsilon_r}{e} \frac{dE(x)}{dx} = p(x) - n(x) - n_t(x) + p_t(x), \quad (2)$$

and the particle-conservation equations

$$\frac{1}{e}\frac{\partial}{\partial x} J_n = -\frac{1}{e}\frac{\partial}{\partial x} J_p = R = R_L + R_{SRH} \quad (3)$$

In these equations, J_n is the electron current, J_p the hole current, $p(x)$ and $n(x)$ represent the density of mobile holes and electrons, $n_t(x)$ and $p_t(x)$ the density of trapped electrons and holes. Furthermore, $E(x)$ is the electric field as a function of position x, and $D_{n,p}$ are the carrier diffusion coefficients, which are assumed to obey the Einstein relation $D_{n,p} = \mu_{n,p} k_B T/e$.[15] The total recombination rate R contains both emissive Langevin recombination R_L and non-radiative trap-assisted (Shockley-Read-Hall, SRH) recombination R_{SRH}.[5] The transport of charge carriers in disordered organic semiconductors can be described by the Extended Gaussian Disorder model (EGDM), that takes into account both the field- and charge carrier concentration dependence of the electron- and hole mobility $\mu_n(n,E,T)$ and $\mu_p(p,E,T)$, respectively.[6]

2.3 Pristine super-yellow PPV PLED

As a starting point for our modelling study, we first investigate the hole transport, electron transport and double-carrier characteristics of a pristine PLED based on super-yellow PPV (SY-PPV). In Figure 1a the hole current in a ITO/PEDOT/SY/Au

hole-only device is shown as a function of voltage for different temperatures. Experimental data were simulated using the drift-diffusion model with EGDM mobility embedded.[7] For the super yellow polymer the hole current can be described with the mobility parameters μ_0 = 600 m^2/Vs, a = 1.6 nm, and σ = 0.14 eV. The hole mobility at zero field and zero density at room temperature can then be calculated as $\mu_0\,(300\ k)$ = 4.8×10^{-12} m^2/Vs. The electron mobility in PPV derivatives is equal to the hole mobility, which has been verified experimentally.[8] Due to the presence of electron traps in PPV derivatives the electron transport is strongly hindered.[9] In order to model the electron current in SY-PPV, a Gaussian energy distribution of traps in the band gap is used. For Gaussianly distributed traps,[10] the relevant parameters are the trap density N_t, the trap depth below the LUMO E_t, and the width of the Gaussian trap distribution σ_t. Using N_t = 1.0×10^{23} m^{-3}, E_t = 0.74 eV, and σ_t = 0.1 eV, the electron current of SY electron-only devices can be well described, as shown in Figure 1b.

To simulate double-carrier PLED devices, two recombination processes need to be considered: the emissive recombination in PLEDs is always of the bimolecular type (Langevin recombination, Equation 4), whereas the non-radiative recombination is trap assisted (Shockley-Read-Hall recombination, Equation 5). [17, 18]

The current and light-output of a SY-PLED are simulated using the charge-transport data of the single-carrier devices, without any additional free parameters (Figure 1c). In order to model the conversion efficiency of the PLED, defined as emitted photons per injected charge carriers, quenching of excitons at the metallic cathode needs to be taken into account.[11] Using an exciton diffusion length of 6 nm, which is typical for PPV derivatives,[12] the voltage dependence of the efficiency can be well described, as shown in Figure 1d. As a result, the numerical device model provides a consistent description of a pristine super yellow PLED.

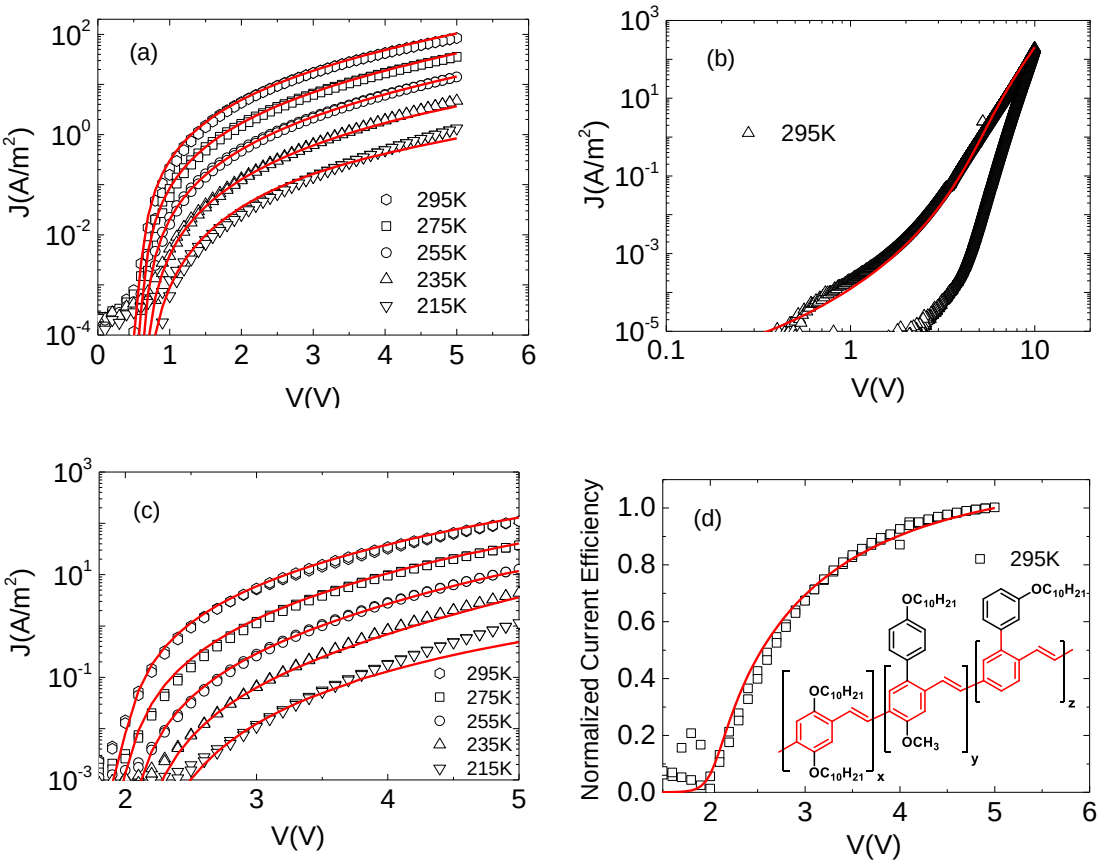

Figure 1. (a) Temperature dependent *J-V* characteristics of hole-only diode of super yellow PPV, (b) *J-V* characteristic of electron-only device of super yellow, (c) Temperature dependent *J-V* characteristics of double-carrier device, (d) Normalized current efficiency of SY-PLED at room temperature (I_{ph}/I_{pled}); inset shows chemical structures of super yellow PPV. All empty symbols represent the experimental data for an active layer thickness of L=100nm, while the solid lines are simulations.

2.4 Aging of a super yellow PLED

As a next step a pristine ITO/PEDOT/SY/Ba/Al PLED with 100 nm polymer thickness has been stresses by applying a constant current density of 10 mA/cm^2. As has been reported before, upon stressing an increase in driving voltage is observed, together with a decrease of the light output *L*, as shown in Figure 2a.

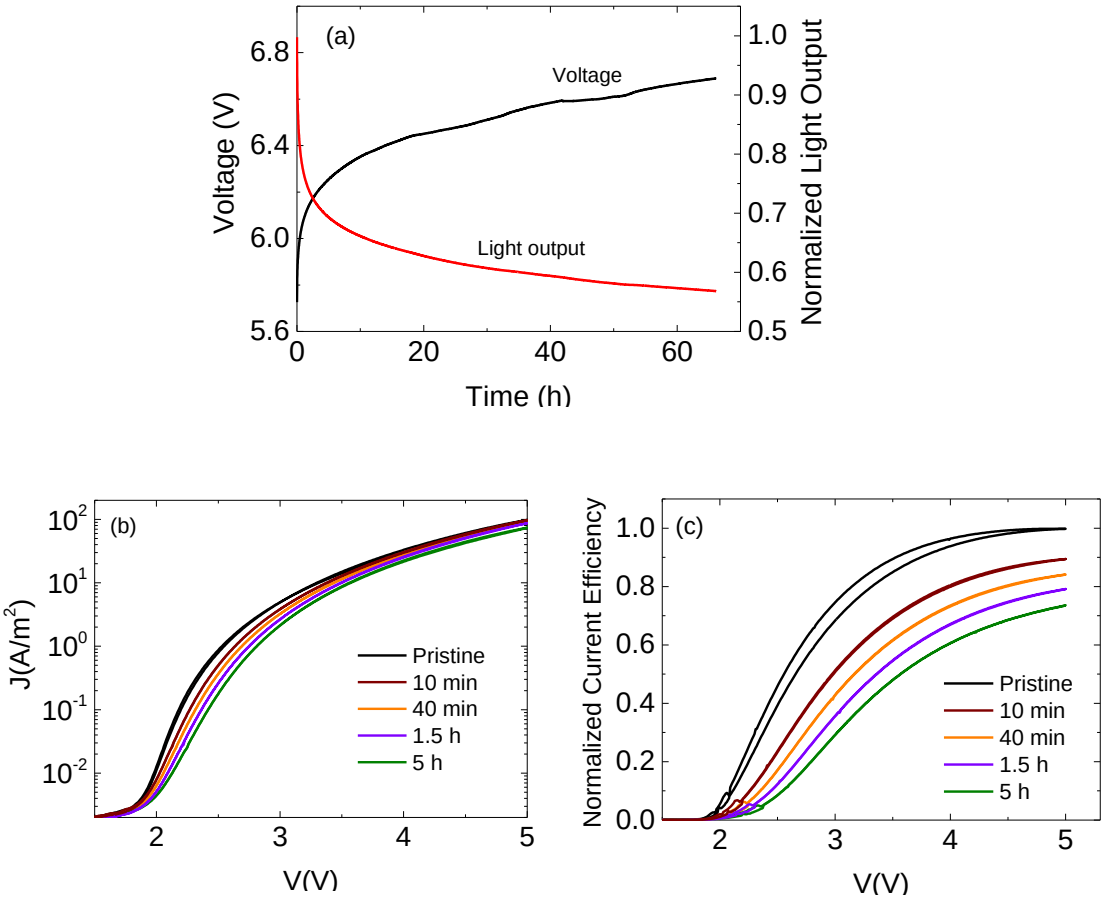

Figure 2. (a) Degradation of a SY-PPV PLED under 10 mA/cm^2. The polymer layer thickness is 100 nm. (b) *J-V* characteristic of PLEDs during aging; (c) Normalized current efficiency of PLEDs during aging.

It is observed that the degradation is much faster in the first few hours as compared to the remaining stress time. Therefore, in the present study we focus on the first 5 hours of stressing. For this purpose, we interrupt the continuous current stress to take a *J-V-L* sweep at a given stress time, then continue the current stress, take again a *J-V-L* sweep at a defined time and so on. In Figure 2b, the changes of the *J-V* characteristics and efficiency of the PLEDs as a function of aging time are depicted. The PLED current in the aged devices shows a decrease mainly at low voltages, but seems to recover at high voltage towards the current of the pristine device. With regard to the efficiency, we observe that the maximum efficiency is lowered and also that the rise of efficiency with voltage becomes slower in degraded devices (Figure 2c).

2.5 Modeling of degraded PLEDs

As mentioned above, based on our understanding about the charge transport and recombination process in a single-layer PLED, the *J-V* characteristics as well as the efficiency can be predicted from the transport parameters of the single carrier devices. The advantage of having a consistent device model is that we can simply vary each parameter (i.e. mobility, traps types, distribution and amount, injection barrier), to individually study its effect on the PLED current and efficiency. In this way, we can discriminate which process plays the most critical role during degradation of a PLED.

2.5.1 Charge carrier mobility

As shown in Figure 2a the degradation of a PLED is characterized by a decrease in light output combined with a voltage increase under a constant driving current. Since PLEDs are space-charge-limited devices, an increase of driving voltage can be the direct result of a mobility decrease. Such a mobility decrease could for example originate from the breaking of conjugated bonds due to a chemical reaction under electrical stress.

To change the mobility in our simulations we only have to change the mobility pre-factor for both charge carriers. As an example, in Figure 3a the mobility pre-factor is decreased from 600 $m^2 V^{-1} s^{-1}$, as used to model the pristine device, to 200 $m^2 V^{-1} s^{-1}$. As expected, the double carrier PLED current decreases. However, from Figure 3b it appears that a decrease of the mobility does not affect the PLED conversion efficiency (exciton/carrier). The reason is that the conversion efficiency in PLEDs is defined as light output divided by current, meaning the numbers of photons emitted per unit time, divided by the number of charges that passed the device in the same time interval. As can be seen from Equation 4 and 5 both the current and recombination pre-factors of radiative Langevin and non-radiative SRH

recombination, respectively, all linearly scale with the mobility. By dividing these rates for current and light output the mobility drops out and the efficiency is mobility independent. As a result, a decrease of the charge carrier mobility is not consistent with the loss of efficiency during degradation.

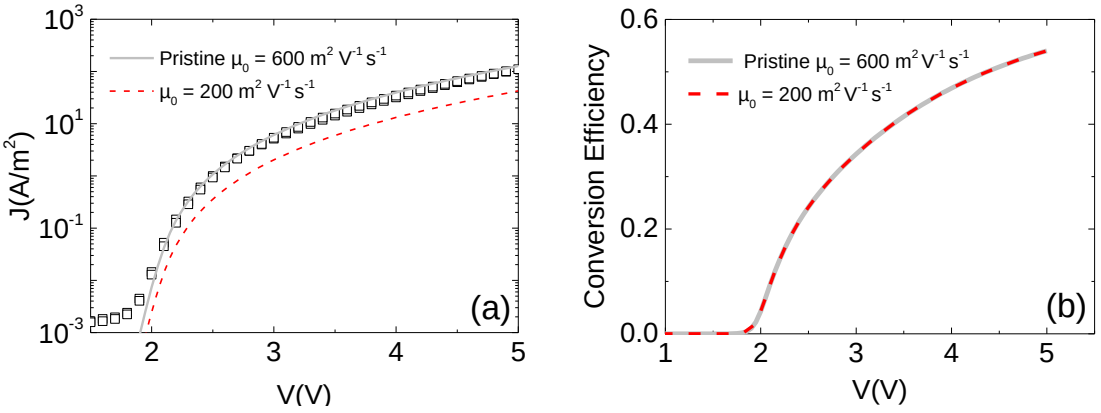

Figure 3. Calculated *J-V* characteristic (a) and conversion efficiency (b) of pristine and aged PLED with μ_0 = 600 m^2 V^{-1} s^{-1} and 200 m^2 V^{-1} s^{-1} respectively. Empty symbols represent the experimental data for an active layer thickness of L=100nm, while the solid lines are simulations.

It should be noted that also an individual change of the mobility parameters as energetic disorder σ or lattice constant a will only lead to changes in the current, but not in device efficiency. Another possibility to explain the voltage increase during current stress would be a change of the charge injection barriers. For hole injection the role of an interface reaction between ITO and PEDOT, or the deterioration of PEDOT itself, have been discussed.[13,14] For electron injection, chemical reactions at the interface between cathode materials as barium or calcium and the polymer were also investigated.[15] In general, it is argued that intrinsic degradation is mainly due to the changes in the bulk of the polymer, and that the electrodes only play a minor role for the device lifetime.[16,17]

Our simulations show (not shown here) that an increase of the injection barrier for either holes or electrons, which reduces the work function difference between the two

electrodes, will lead to a reduction of the built-in voltage (V_{bi}). This reduced V_{bi} will lead to a shift of the complete *J-V* characteristic of the PLED to lower voltage. This shift should be especially well visible in the diffusion dominated current regime $V < V_{bi}$. Such a shift due to a decrease of V_{bi} is not observed for degraded devices, confirming the absence of the formation of injection barriers during degradation.

2.5.2 Electron traps

It has been demonstrated in the past that hole-only devices do not degrade under electrical stress. [2, 12, 13] As a result, it was concluded that electron transport plays an important role for the PLED degradation. It was postulated that the electron transport degrades during electrical fatigue due to the formation of additional electron traps. To check the effect of the formation of electron traps during degradation on the performance of PLEDs we gradually increased the density of e-traps, while keeping the trap energy distribution and depth the same as for the pristine device. From Figure 4b, we observe that the device efficiency decreases with increasing amount of electron traps. A higher density of traps will lead to an increase of the non-radiative SRH recombination, as can be seen from Equation 5. In contrast, more electron traps will also lead to a reduction of the density of free electrons and therefore to a decrease of the radiative Langevin recombination. This shift of balance between the radiative and non-radiative recombination is then responsible for the decreased efficiency of the PLED. However, the effect of an increased amount of electron traps on the PLED current is relatively weak as seen in Figure 4a. With increasing amount of electron traps, the current will decrease only a bit and for sufficiently high electron trap concentration the PLED current collapses on the hole current. Further increase of the amount of traps does not influence the current. As pointed out by Rosenberg and Lampert,[18] for the limiting case of infinite recombination the bipolar PLED current is just equal to the sum of the electron and hole current. When the electron current is already significantly smaller than the hole current, as is the case in PLEDs, a further

decrease in its magnitude will not affect the PLED current. In that case PLED current will just be equal to the hole current, nearly independent of the amount of electron traps.

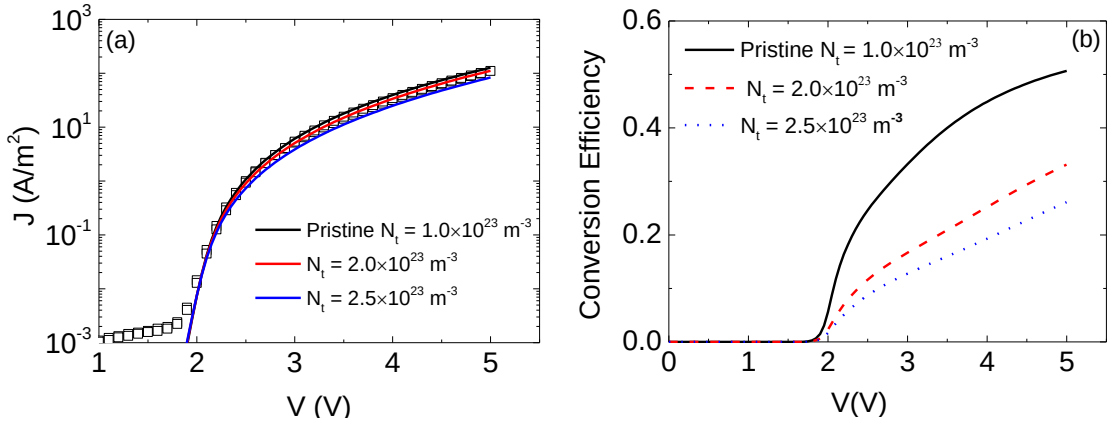

Figure 4. Calculated *J-V* characteristic (a) and conversion efficiency (b) of pristine and aged PLED with increasing electron traps density. Empty symbols represent the experimental data for an active layer thickness of L=100nm, while the solid lines are simulations.

From an experimental point of view, we can now compare the hole current of the pristine device with the bipolar current of the degraded device as shown in Figure 5. We note that for a correct comparison, the applied voltage for the hole-only device has to be corrected for the built-in voltage of the PLED. It appears from Figure 5 that the PLED current for the SY-PPV can reach values far below the hole current of a pristine device, when the devices are stressed for a sufficiently long time. This result shows that the formation of electron traps alone cannot be responsible for the observed degradation phenomena of the PLED. In fact, the only possible explanation for this observation is that hole transport must degrade during device aging. A similar conclusion was drawn by Stegmaier et al., [12] who observed a decrease of hole transport in aged PLEDs by TOF measurements.

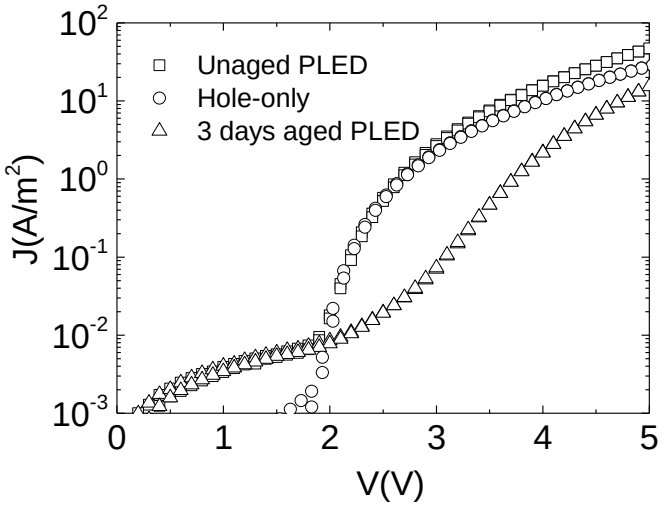

Figure 5. *J-V* characteristic of super yellow polymer (120 nm) based hole-only device, pristine PLED and 3 days aged PLED under 10 mA/cm^2. The voltage of the hole-only device has been adjusted so that its built-in voltage coincides with the built-in voltage of the PLED.

2.5.3 Hole traps

It was already demonstrated that a reduction of the hole mobility is not consistent with the experimental observations. Another mechanism that reduces the hole transport during electrical stress is the formation of hole traps.

For the introduction of hole traps we postulate that they are formed homogeneously throughout the active layer. Furthermore, we assume that they are Gaussianly distributed in energy, similar to the electron traps. We note that by setting the width of the distribution to a small value,[10] also discrete single level traps can be simulated.

Introduction of hole traps P_t in the current equations alone is not sufficient to simulate their effect on the PLED current and efficiency. The formation of hole traps will also lead to an additional loss process, namely the non-radiative recombination of free electrons with trapped holes. Such a process has until now never been considered in a

PLED. When both electron (N_t) and hole traps (P_t) are present in the semiconductor, the total SRH recombination will be the sum of recombination of free holes with trapped electrons (SRH_E) and recombination of free electrons with trapped holes (SRH_P). The total SRH pre-factor is then given by:

$$B_{SRH} = B_{SRH\_E} + B_{SRH\_P} = C_n C_p \left(N_t + P_t\right) / \left[C_n (n + n_1) + C_p (p + p_1)\right] \quad (9)$$

As input parameters for the simulations, we set the depth of the hole traps E_{pt} = 0.6 eV, and their distribution width σ_p = 0.1 eV. Then we increase the hole traps density from 0 for the pristine device to 2×10^{23} m^{-3} to study their effect on *J-V* and PLED efficiency. The corresponding calculated *J-V* curves and corresponding efficiency evolution are shown in Figure 6.

We observe that, as expected, the current decreases with increasing amount of hole trap density, since the hole transport dominates the PLED current. This reduction is especially strong at lower voltages. At higher voltages the PLED current partially recovers to the pristine value, since then the large density of injected charges at high voltage will fill all the traps and recover the current. In parallel, a decrease of the efficiency is also observed, due to the additional non-radiative recombination of free electrons with trapped holes. As a conclusion, an increased amount of hole traps simultaneously gives rise to a decrease of the PLED current, especially at low voltages, and a reduction of the efficiency. These results are qualitatively in agreement with the observations made on degraded devices.

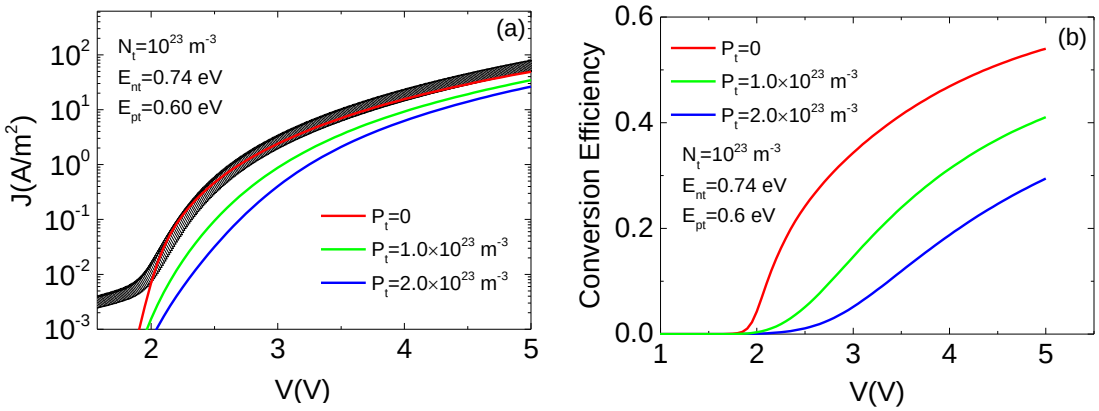

Figure 6. Calculated *J-V* characteristic (a) and conversion efficiency (b) of pristine and aged PLED with increasing hole traps density. Empty symbols represent the experimental data for an active layer thickness of L=120nm, while the solid lines are simulations.

As a next step, we test if we can also quantitatively link the experimental observations to the simulations. Figure 7 shows the degradation of a SY-PPV PLED with 120 nm polymer thickness under 10 mA/cm^{-2} for 3 hours and 15 hours. It again shows a fast decrease of both current and efficiency in the first hours of current stress. For the simulation of the pristine device, the hole-trap density is set to zero. The voltage dependence of the current of the degraded devices is influenced by both the depth of hole traps and the width of their distribution. By using 0.6 eV for the trap depth (above the HOMO of SY) and a Gaussian distribution width of σ = 0.1 eV the best agreement is obtained. In that case, we find a hole trap concentration P_t of 1.4×10^{23} m^{-3} for the 3 hours aged SY-PPV PLED and 2.1×10^{23} m^{-3} for the 15 hours aged one. Now, with the PLED current fitted, there is no free parameter left to describe the PLED efficiency. Figure 7b demonstrates that with this set of parameters the PLED current and efficiency are simultaneously described.

We note that in these simulations we have kept all other parameters constant, equal to the ones of the pristine device. Furthermore, we investigated whether a joint increase

of hole and electron traps would be able to explain the experimental data as well. Additional electron traps mainly affect the light-output, whereas hole traps have a strong effect on the current. Simulations showed that a joint increase of electron and hole traps to fit the current leads to an underestimation of the light-output. Summarizing, the formation of hole traps quantitatively explains both the increase of voltage and the decrease of efficiency of a PLED under constant current stress.

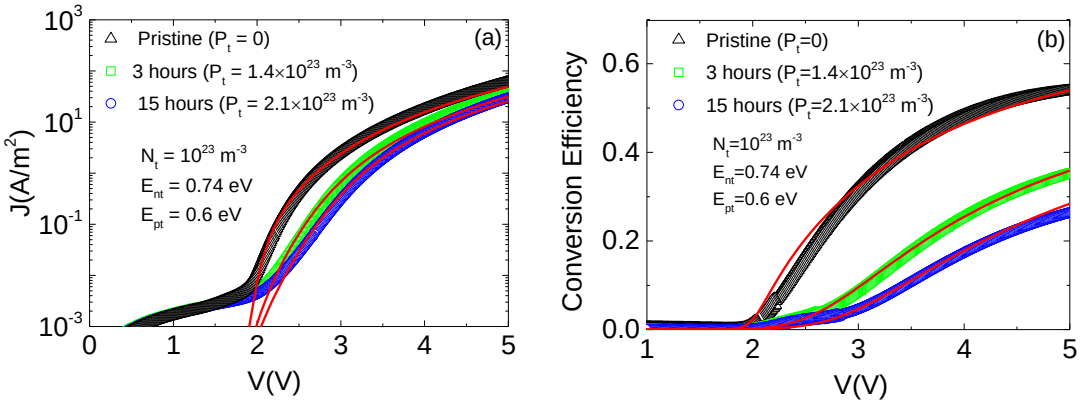

Figure 7. *J-V* characteristic (a) and conversion efficiency (b) of pristine and 3 hours and 15 hours aged PLED under 10 mA/cm^2 compared with simulation by increasing hole traps density. All empty symbols represent the experimental data for an active layer thickness of L=120 nm, while the solid lines are simulations.

2.5.4 Charge distribution and recombination profile

As a next step we evaluate the consequences of the occurrence of hole traps for the device operation of a degraded PLED. The device simulations provide us the spatial distributions of electric field, free and trapped charges and the Langevin recombination profile *n(x)p(x)*. In Figure 8 we show the calculated charge carrier profiles (8a) and the recombination profile (8b) for a pristine and a degraded PLED. The formation of hole traps leads to a decreased free hole density p(x) in the device. Furthermore, with increasing amount of hole traps the spatial distribution of free holes

becomes increasingly confined to a region close to the anode. As a result, the recombination profile *n(x)p(x)*, which in a pristine device is confined close to the cathode due to electron trapping, will start to spread out and shift in the direction of the anode upon degradation. In the calculations, quenching by the electrodes in a 10 nm region next to the electrode has been taken into account.[25] As shown in Figure 8b, the emission zone broadens during degradation. Due to the reduction of free holes the intensity of Langevin recombination will be strongly reduced, as shown in Figure 8b for using $P_t = 2.1\times10^{23}$ m^{-3}, E_{pt} = 0.6 eV, and σ_{pt} = 0.1 eV as hole trapping parameters. Furthermore, the recombination of free electrons with trapped holes introduces an additional non-radiative loss process. Combinations of both processes are then responsible for the efficiency loss in a degraded PLED. In Figure 9 the relative evolution of the recombination and loss processes in a pristine and degraded PLED are compared as a function of voltage. We note that due to the shift of the recombination zone the quenching of excitons by the electrodes does not play a significant role in degraded PLEDs.

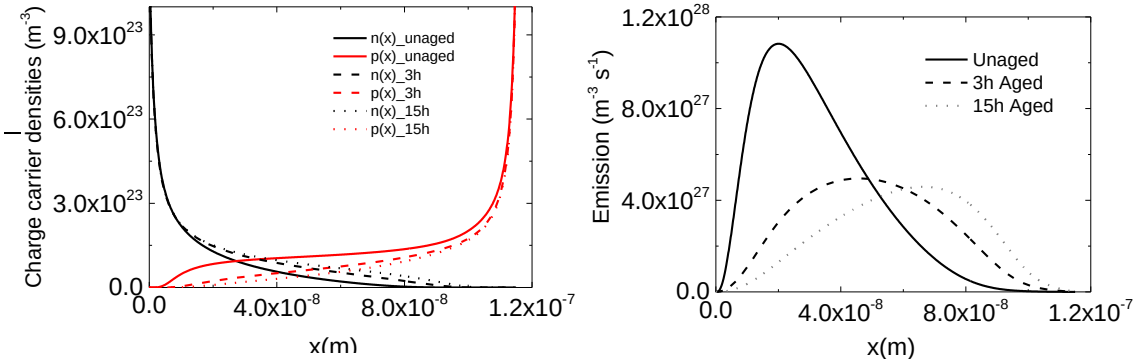

Figure 8. Calculated charge carrier distribution before (solid line) and after 3 hours (dash line) and 15 hours (dot line) aging (a); Calculated emission zone before (solid line) and after 3 hours (dash line) and 15 hours (dot line) aging (b); all devices were aged under 10 mA/cm^2.

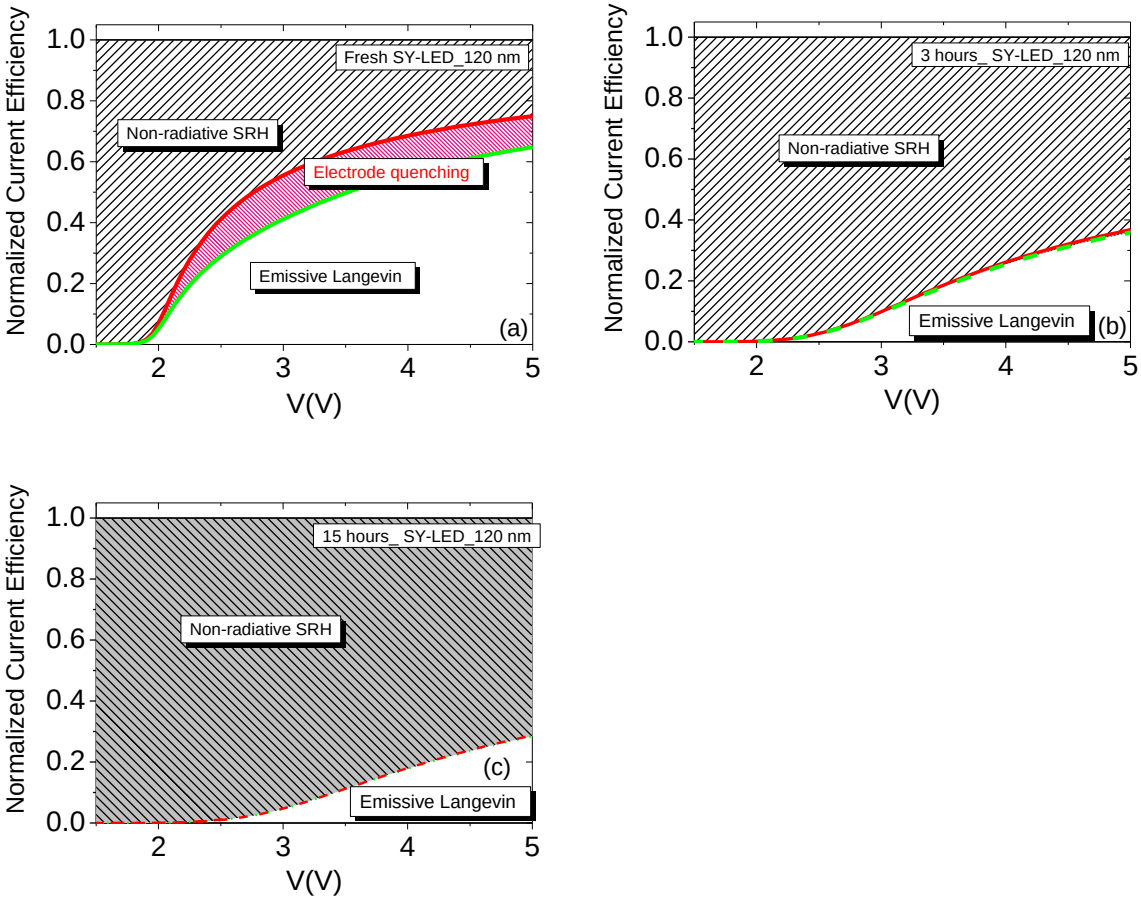

Figure 9. Calculated contributions of the two loss process in a 120 nm SY-PPV PLED before (a) and after (b) 3 hours and (c) 15 hours aging; all devices were aged under 10 mA/cm^2. Green lines (solid and dash) show the emissive Langevin recombination. The hashed areas between red and green lines indicate the efficiency loss by electrode quenching. While the black dashed areas indicate the efficiency loss by non-radiative SRH recombination.

We note that for small molecule OLEDs it was shown that a broadening of the emission zone leads to an improvement in the lifetime.[19] As a result, the broadening of the recombination zone upon formation of hole traps might act as a self-limiting process that slows down degradation at longer times.

2.6 Hole transport measurement upon degradation

From the simulations it was concluded that the hole transport will degrade upon PLED aging due to the formation of hole traps. In order to investigate the hole transport in a degraded device we conducted transient electroluminescence (TEL) measurements.[3] Unlike TOF, which typically requires a thick (~μm) semiconductor film, TEL can be easily used in conventional PLEDs with ~100 nm polymer thickness. In a TEL measurement, a rectangular voltage pulse is applied to the PLED with varying length. In a pristine PLED, after application of a voltage, holes will travel form the anode to the cathode with a finite transit time τ. When the fastest holes reach the recombination zone, which is near the cathode due to electron trapping, light output begins. Thus, the delay time τ_d between the onset of pulse and light output is a measure for the hole transit time.

Figure 10 shows the results from TEL measurements on pristine- and aged SY-PPV PLEDs. It appears that during aging the transit time τ gradually increases with prolonged aging time. This is consistent with our simulation results that hole transport will be slowed down due to the formation of hole traps. However, we note that a quantitative interpretation of the hole transit time is not straightforward. First, the hole transport in PPV derivatives is highly dispersive, such that the transit time is governed by the fastest carriers. These fastest carriers are typically the carriers that are not being trapped. However, it has been shown by Fleissner et al. that deep traps indeed will lead to an increase of the measured transit time.[20] Secondly, the recombination zone shifts during aging from the cathode side more to the center of the PLED. Thus, for an aged device the holes typically have to travel only half of the device thickness to generate light. However, the observed increase of the hole transit time confirms the decrease of the hole transport for an aged PLED.

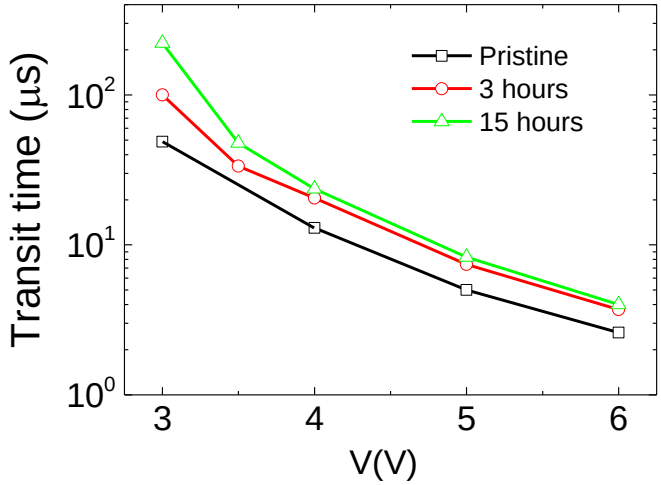

Figure 10. Transit time of hole transport in SY-PPV PLEDs as a function of applied voltage obtained from TEL measurement with prolonged device aging for 3 hours and 15 hours at 10 mA/cm^2.

2.7 Conclusion

In conclusion, we have analyzed possible mechanisms for PLED degradation by device modelling. By individually changing the device parameters, we have found that a change of mobility, an increase of electron traps or the increase of injection barriers, cannot explain the experimentally observed phenomena during degradation. The strong decrease of PLED current, which even gets lower than the hole current in a pristine device, can only be explained by degradation of the hole transport. The generation of hole traps during degradation simultaneously explains the decrease of the *J-V* characteristic and efficiency of degraded PLEDs. The formation of hole traps also induces a shift of the recombination profile towards the anode, thereby reducing the exciton quenching by the cathode. The degradation of the hole transport was confirmed by transient electroluminescence measurements.

Our simulations have identified the formation of hole traps as the main mechanism for the voltage increase and efficiency loss of degraded PLEDs. This result will enable us in a future study to evaluate how the formation of hole traps depends on the stress

conditions, and with which of the processes in the PLED it correlates. This information will help us to unravel the nature of the hole traps and the mechanism for hole trap formation, paving the way towards stable PLEDs.

Experiments

1. Materials and devices

The polymer used as a reference in this work is a poly(*p*-phenylene vinylene) (PPV) copolymer, known as 'super yellow' (SY-PPV,Merck AG). Its chemical structure is shown in Figure 1d (inset). To fabricate devices, SY-PPV was dissolved in toluene and spin-coated on a glass/ITO/PEDOT:PSS substrate. The layer thickness of SY-PPV is in the range of 100 to 120 nm. The cathode was then thermally evaporated on top of the polymer (chamber pressure 10^{-7} mbar). The corresponding device architectures used in this study are ITO/PEDOT/SY/Au for hole-only devices and ITO/PEDOT/SY/Ba/Al for PLEDs. For electron-only devices, patterned electrodes of Al were deposited on glass by thermal evaporation to form the anode, resulting in a structure of Al_2O_3/SY/Ba/Al. All devices were measured in nitrogen atmosphere, and stressed under a constant current density of 10 mA/cm^2 in the aging tests.

2. Transit time measurement

To measure the transit time (τ) of charge carriers before and after PLED aging, an ITO/PEDOT/SY/Ba/Al PLED with an active layer thickness of 120 nm was used as a test device. An Agilent 8114A pulse generator was utilized to input a voltage pulse, resulting in a light output pulse. The width of the voltage pulse τ_{pulse} was increased from 2 μs to 600 μs, and the pulse amplitudes were varied gradually from 3 V to 6 V with a 0.5 V step. The pulse period was set to be 1 ms. The integrated light output (l_{out}) is measured by a Keithley 6514 electrometer in current mode. When $\tau_{pulse} >> \tau$, a linear relation between l_{out} and τ_{pulse} will be obtained, the intercept of the linear part with the τ_{pulse} axis is corresponding to τ.

Reference

[1] M. Kuik, G. J. A. Wetzelaer, H. T. Nicolai, N. I. Craciun, D. M. De Leeuw, P. W. Blom, *Advanced Materials* **2014**, *26*, 512.

[2] Q. Niu, G. J. A. Wetzelaer, P. W. Blom, N. I. Crăciun. *Advanced Electronic Materials* **2016**, *2*.

[3] P. W. M. Blom, M. C. J. M. Vissenberg. *Physical Review Letters* **1998**, *80*, 3819.

[4] A. Gassmann, S. V. Yampolskii, A. Klein, K. Albe, N. Vilbrandt, O. Pekkola, Y. A. Genenko, M. Rehahn, H. von Seggern. *Materials Science and Engineering: B* **2015**, *192*, 26.

[5] M. Kuik, L. J. A. Koster, G. A. H. Wetzelaer, P. W. M. Blom. *Physical Review Letters* **2011**, *107*, 256805.

[6] W. Pasveer, J. Cottaar, C. Tanase, R. Coehoorn, P. Bobbert, P. Blom, D. De Leeuw, M. Michels. *Physical review letters* **2005**, *94*, 206601.

[7] L. J. A. Koster, E. C. P. Smits, V. D. Mihailetchi, P. W. M. Blom. *Physical Review B* **2005**, *72*, 085205.

[8] Y. Zhang, B. de Boer, P. W. M. Blom. *Physical Review B* **2010**, *81*, 085201.

[9] M. Mandoc, B. de Boer, G. Paasch, P. Blom. *Physical Review B* **2007**, *75*, 193202.

[10] H. Nicolai, M. Mandoc, P. Blom. *Physical Review B* **2011**, *83*, 195204.

[11] M. Kuik, L. J. A. Koster, A. G. Dijkstra, G. A. H. Wetzelaer, P. W. M. Blom. *Organic Electronics* **2012**, *13*, 969.

[12] D. E. Markov, C. Tanase, P. W. M. Blom, J. Wildeman. *Physical Review B* **2005**, *72*, 045217.

[13] F. So, D. Kondakov. *Advanced Materials* **2010**, *22*, 3762.

[14] J. S. Kim, P. K. H. Ho, C. E. Murphy, N. Baynes, R. H. Friend. *Advanced Materials* **2002**, *14*, 206.

[15] H. Aziz, G. Xu. *Synthetic Metals* **1996**, *80*, 7.

[16] J. Scott, J. Kaufman, P. Brock, R. DiPietro, J. Salem, J. Goitia. *Journal of Applied Physics* **1996**, *79*, 2745.

[17] I. D. Parker, Y. Cao, C. Y. Yang. *Journal of Applied Physics* **1999**, *85*, 2441.

[18] L. M. Rosenberg, M. A. Lampert. *Journal of Applied Physics* **1970**, *41*, 508.

[19] T.-H. Han, Y.-H. Kim, M. H. Kim, W. Song, T.-W. Lee. *ACS applied materials & interfaces* **2016**, *8*, 6152.

[20] A. Fleissner, H. Schmid, C. Melzer, H. von Seggern. *Applied Physics Letters* **2007**, *91*, 242103.

Chapter 3 Degradation of polymer light-emitting diodes by hole traps formation

As discussed in Chapter 2, the voltage drift of a polymer light-emitting diode (PLED) driven at constant current is caused by the formation of hole traps. By analyzing the voltage drift with a numerical device model, we demonstrate that the hole trap concentration initially increases linearly with time (burn-in) and subsequently grows with the square-root of time. This transition is governed by the statistics between free and trapped holes. With the amount of hole traps known, the light output of the PLED can be predicted as a function of aging time. The good agreement between predicted and measured light-output shows that the mechanism for the efficiency decrease under stress is the additional non-radiative recombination between free electrons and trapped holes. The observed trap formation rate is consistent with exciton-free hole interactions as the main mechanism behind PLED degradation. Revelation of this degradation mechanism enables us to unify the degradation of a series of poly(p-phenylene) derivatives based PLEDs.

3.1 Introduction

In the previous chapter, as a first step to discriminate between the various proposed degradation mechanisms numerical simulations were performed on the device characteristics of pristine and degraded PLEDs. It was found that the device characteristics, current density and light-output as a function of voltage, of degraded PLEDs are consistent with the formation of hole traps.[1] The identification of hole trap formation as a main cause for degradation enables us now to quantitatively investigate the aging-time dependence of the hole trap formation as well as its dependence on stress conditions. Using numerical simulations, the rate of hole-trap generation is directly determined from the voltage increase during stress. The light-output of the PLED can then be predicted as a function of aging time and is in good agreement with the experimental observation. This demonstrates that the additional non-radiative recombination of free electrons with trapped electrons is responsible for the loss in light output and efficiency upon aging. The observed hole trap formation rate is consistent with a mechanism based on interaction between excitons and (positive) polarons.

3.2 Hole trap generation as a function of aging time

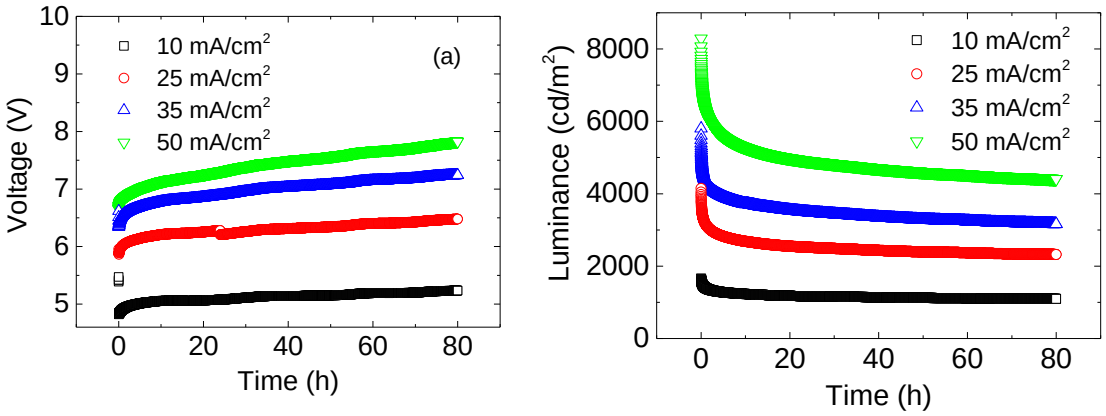

Figure 1. (a) Voltage and (b) luminance of SY-PPV based PLEDs aged under four different current densities: 10, 25, 35, and 50 mA/cm^2; the thickness of the SY-PPV layer is 100 nm.

PLEDs with a 100 nm SY-PPV layer thickness were aged at four different current densities of 10, 25, 35 and 50 mA/cm^2, respectively. For pristine PLEDs, these current densities correspond to luminance of 1658, 4144, 5803, and 8289 cd/m^2. The voltage and luminance were recorded as a function of aging time (Figure 1). For the devices stressed at higher current densities, the voltage drift is stronger and a faster descent of the luminance was observed. To link the voltage increase to the formation of hole traps a numerical PLED device model was used, which includes electron trapping and a field- and density-dependent free carrier mobility.[2] The recombination in the PLED is governed by a competition between emissive Langevin-type recombination and non-radiative trap-assisted (Shockley-Read-Hall, SRH)[3] recombination. The transport parameters of SY-PPV were obtained from pristine hole-only and electron-only devices.[1] Using these parameters, which also define the rates of Langevin and SRH recombination,[2] the *J-V* characteristics and efficiency of pristine super yellow LEDs can be described over the full voltage range. For PLEDs under stress, the generation of hole traps will increase the amount of trapped immobile

charges in the device, causing the voltage to rise in order to maintain a constant current. Additionally, the formation of hole traps will lower the PLED efficiency by additional non-radiative recombination of free electrons with trapped holes. As a first step, we assume that the hole traps are homogenously generated in the active layer. With this assumption, for any driving voltage *V(t)*, the amount of corresponding hole traps $P_t(t)$ that is required to maintain a constant current can be calculated. From the recorded voltages, as displayed in Figure 1, the density of hole traps $P_t(t)$as a function of aging time are calculated and plotted in Figure 2a. On a double-logarithmic scale, after an initial steeper increase, a linear relation between $P_t(t)$ and aging time is observed for all aging conditions, with a slope that is approximately equal to 0.5. Furthermore, in this regime, the density of hole traps generated after a certain aging time is proportional to the current density, as shown in Figure 2b. As a result, the formation of hole traps as a function of aging time can be described as:

$$P_t(t) = \alpha \times J \times \sqrt{t} \qquad (1)$$

where α is a proportionality constant, J the aging current density and t the aging time. With such an empirical expression, the generation of hole traps during SY-PPV PLED degradation can be predicted for any given driving current. We note that this expression shows that the hole trap formation is not proportional to the total amount of charge passed through the PLED upon aging, which is given by $Q=J\times t$.

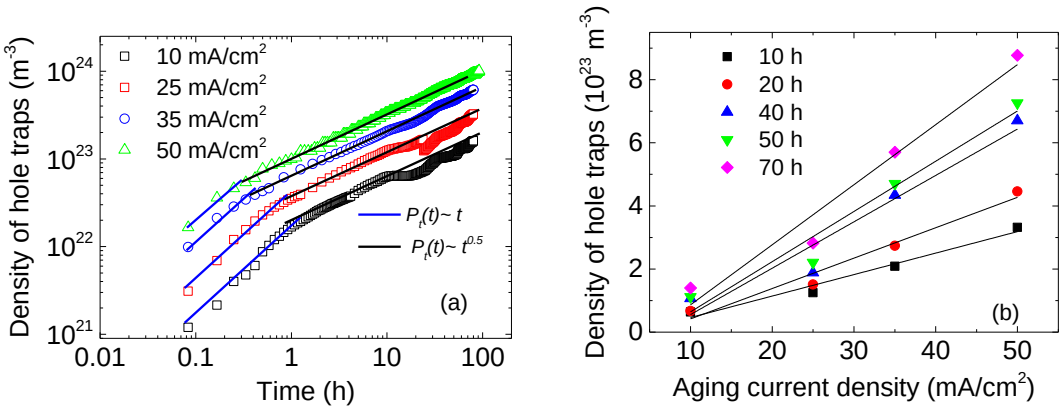

Figure 2. (a) Density of hole traps formed during degradation of SY-PPV PLEDs under four different current densities: 10, 25, 35, 50 mA/cm^2. Symbols are experimental data, lines with slope 0.5 (black) and slope 1 (blue) are a guide to the eye. (b) Density of hole traps as a function of aging current density for various aging periods. The thickness of the SY-PPV layer is 100 nm.

Furthermore, when applying a higher aging current density (50 mA/cm^2) it is observed that the voltage first slightly decreases to a minimum value in the first minutes, and afterwards increases smoothly with aging time (Suppl. Info, Figure S1). Such a voltage decrease at short times is the result of an increase of the internal PLED temperature, due to Joule heating. [4,5] Due to a temperature rise, the charge-carrier mobility increases and thereby lowers the driving voltage at constant current. Using our simulations, we find that the internal PLED temperature rise at 50 mA/cm^2 only amounts to 5 K, which is accounted for in the analysis of the voltage drift versus aging time (see Suppl. Info, Figure S1).

3.3 Luminance degradation of PLEDs

From the recorded driving voltage, the density of hole traps as a function of aging time is obtained. Using numerical simulations, the luminance of the PLED, given by the decay of excitons formed by Langevin recombination, at the corresponding aging

time can be independently calculated. The predicted decrease of the Langevin recombination rate with aging time can then be directly compared to the measured luminance decay of the PLED. In figure 3, the experimental luminance decays of 100 nm SY-PPV PLEDs aged under 10, 25, 35 and 50 mA/cm^2 are plotted, together with the simulated descent of the Langevin recombination. We observe that the luminance decay and predicted Langevin recombination are in very good agreement for all aging conditions. This result indicates the mechanism for the efficiency loss of PLEDs upon aging: the formation of hole traps decreases the density of free holes and introduces additional non-radiative recombination of free electrons with trapped holes.[1]

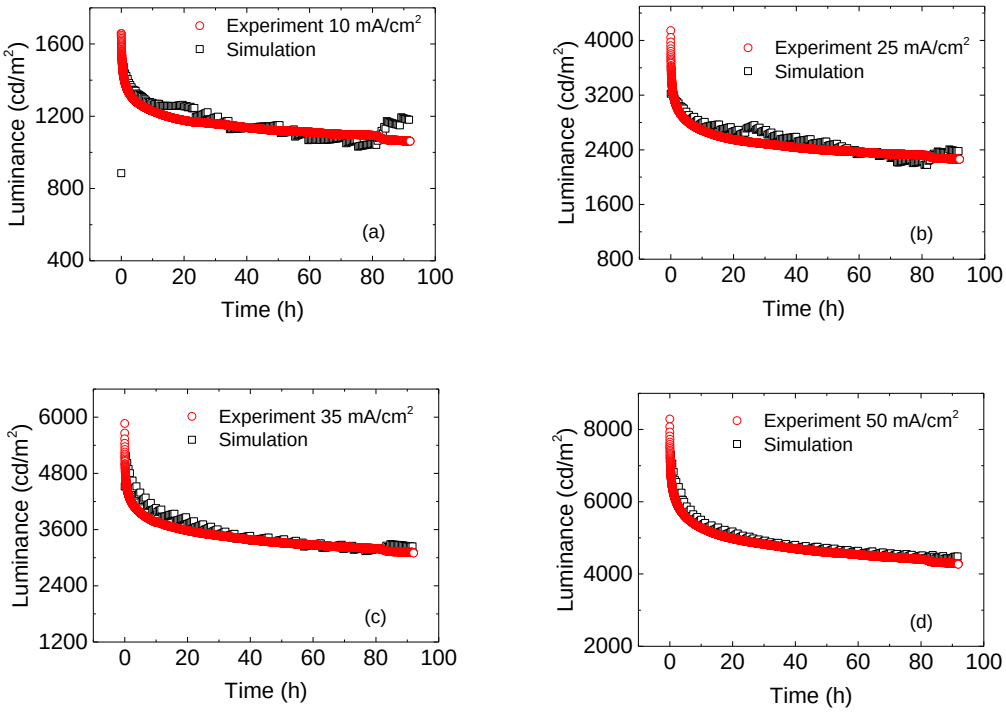

Figure 3. Experimental luminance (red circles) and normalized rate of Langevin recombination (black squares) of SY-PPV PLEDs aged under four different current densities: (a) 10 mA/cm^2, (b) 25 mA/cm^2, (c) 35 mA/cm^2, and (d) 50 mA/cm^2; The thickness of the SY-PPV layer is 100 nm.

In pristine PLEDs, the transport is dominated by holes, since the electron current is strongly limited by traps that are already present in the pristine material. [6] Upon

degradation, additional hole traps are formed, meaning that the charge transport becomes more balanced. After sufficient aging, the amount of hole traps will exceed the amount of initial electron traps and the transport in the PLED will become electron dominated. In PPV derivatives, the electron transport is typically characterized by a strong voltage dependence of the electron current ($J \sim V^6$), which is governed by the energetic distribution of the electron traps.[6,7] In Figure 4, the *J-V* characteristics of a SY-PPV PLED of 100 nm thickness aged at 25 mA/cm^2 for 973 hours is shown. For this PLED, the luminance has decreased to 36% of its initial value. The *J-V* characteristics of the aged PLED are then compared to the *J-V* of pristine electron-only devices with the same polymer thickness (Figure 4.). We observe that the PLED current is still slightly higher than the pristine electron current, but both have the same slope on a double logarithmic plot. As a result, the degraded PLED current and electron current exhibit the same power-law dependence on voltage. This result shows that the current in such a strongly-degraded PLED is electron dominated. The fact that the PLED current is slightly higher than the electron-only current originates from the fact that in a PLED also positive holes are present that neutralize the negative charge of the electrons, such that more electrons are electrostatically allowed at the same bias voltage. It should be noted that when also electron traps would be formed upon degradation of the PLED, the shape of the electron trap distribution and therefore also the voltage dependence of the electron current would change. The equal voltage dependence of a degraded PLED and electron current further supports that the formation of hole traps is the dominant process during PLED degradation.

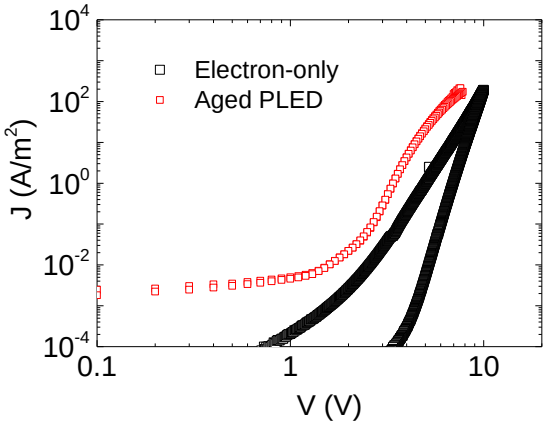

Figure 4. *J-V* characteristics of aged SY-PPV PLED current (red square) compared with electron current measured in an electron-only device (black square). The PLED is aged under 25 mA/cm^2 for 973 hours. The thickness of the SY-PPV layer in both devices is 100 nm.

An assumption in our model is that the generation of hole traps is uniformly distributed through the active layer. In space-charge-limited devices like PLEDs, the carrier density, electric field, and recombination profile are dependent on the position in the active layer. However, in deriving the Mott-Gurney law for space-charge-limited currents, only a small error of 9/8 is made when average carrier densities and electric field are used instead of taking their position dependence into account.[8] So by using average values instead of a spatial distribution, the error is relatively small. The fact that the predicted light-output under aging is in good agreement with experiments is already an indication that a homogenous (average) trap distribution is a good approximation. To further check whether such an assumption is valid for the degradation analysis, PLEDs with different layer thicknesses of SY-PPV were fabricated and aged under the same constant current density of 10 mA/cm^2. Since the current in PLEDs is space-charge limited, the current density scales proportional to the reciprocal of semiconductor layer thickness to the third power. Thus, in order to maintain the same current, a PLED with a thicker active polymer layer requires a higher driving voltage, as shown in Figure 5a. As also observed by Parker et al.[9] the voltage drift for thicker PLEDs is more pronounced as compared to

thinner devices, but this was not further quantitatively addressed. Here, the resulting hole trap densities $P_t(t)$ were subsequently modeled from the dependence of voltage $V(t)$ on aging time for various PLED thickness, as shown in Figure 5b. It is demonstrated that the derived hole trap densities $P_t(t)$ versus time for various PLED thickness coincide on one single curve, which after a few hours is again characterized by a slope of approximately 0.5, consistent with the results shown in section 2.1. As a result, the degradation analysis is independent on PLED thickness, showing that a homogenous distribution of hole traps, representing the average hole trap density in the aged semiconductor layer, is a valid approximation.

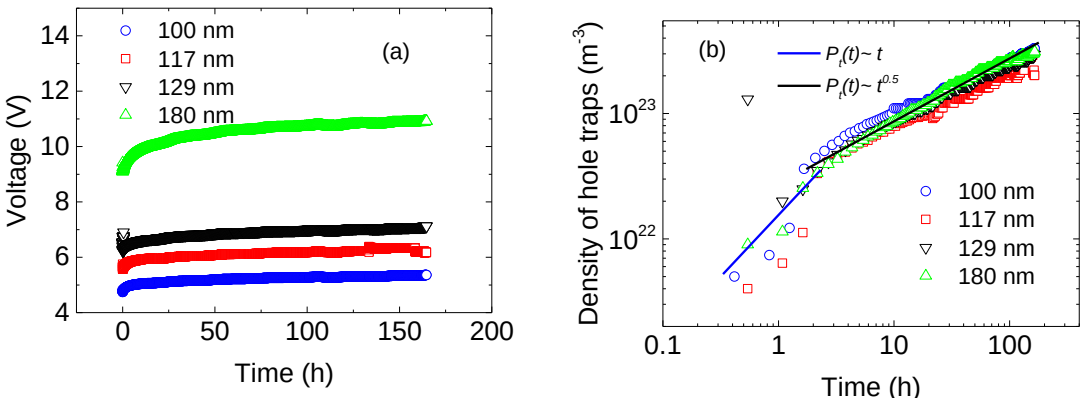

Figure 5. (a) Voltage of PLEDs with different SY-PPV layer thicknesses aged at 10 mA/cm^2 . (b) Density of hole traps formed during degradation of LEDs with different SY-PPV layer thicknesses aged at 10 mA/cm^2.

3.4 Origin of hole trap formation

An important question is how to correlate the observed hole trap formation under aging, given by $P_t(t)=\alpha \times J \times \sqrt{t}$, to a physical degradation mechanism. For organic LEDs based on evaporated small molecules, chemical degradation of the emitting molecules due to bond cleavage is considered as an important degradation mechanism.[10,11] The resulting radical fragments then react to degradation products that result in non-radiative recombination centers. It has been demonstrated by Giebink et al. that the luminescence loss and voltage rise of phosphorescent OLEDs under aging can be modelled by the formation of non-radiative recombination centers due to exciton-polaron annihilation interactions.[10] The model calculations showed a nearly linear increase of the amount of defects with time. From a combination of current displacement and time-resolved electroluminescence, Schmidt et al.[12] identified two mechanisms for the decay in light output of phosphorescent OLEDs under current stress. Next to a decrease in radiative quantum efficiency of the triplet emitter due to triplet exciton-polaron annihilation, also additional non-radiative decay pathways were identified. In contrast to PLEDs, the phosphorescent OLEDs have a complex device structure with a variety of layers and compounds, which complicates a quantitative analysis of the degradation effects. For a single layer PLED, as shown above, a quantitative determination of the amount of created defects as a function of aging time can be directly obtained from the voltage drift. From the observed aging time-dependence of the amount of hole traps, given by Equation 1, it follows directly that the rate of hole trap formation is given by:

$$\frac{dP_t(t)}{dt} = \frac{\alpha^2 J^2}{2P_t(t)} \qquad (2)$$

Contrary to the model proposed by Silvestre et al., who assumed that the rate of defect formation was proportional to the aging current density,[13] equation 2 shows that the rate of defect formation in PLEDs depends quadratically on the driving current density.

This derived rate for hole-trap formation can be rationalized as follows: in the bias

range considered here, the amount of excitons created by Langevin recombination per unit time *L(t)* is proportional to the current density *J*. The Langevin recombination rate is given by [14]

$$R_L = \frac{e}{\varepsilon_0 \varepsilon_r}(\mu_n + \mu_p)np \qquad (3)$$

with μ_n and μ_p the electron and hole mobility, respectively, *e* the electronic charge, $\varepsilon_0\varepsilon_r$ the dielectric constant and *n* and *p* the density of free electrons and holes. During aging, additional non-radiative recombination of free electrons with trapped holes occurs. This rate can be approximated by [15]

$$R_{SRH} \approx \frac{e}{\varepsilon_0 \varepsilon_r}\mu_n P_t n \qquad (4)$$

As a result, *L(t)* during stress has to be corrected with an efficiency factor representing the fraction of bimolecular recombination with regard to the total recombination:

$$L(t) \propto J\frac{R_L}{R_L + R_{SRH}} \approx J\frac{p(t)}{p(t)+P_t(t)} \qquad (5)$$

with *p(t)* the average density of free holes as a function of aging time.

Using equation (5) the product of the exciton-generation rate and the free hole density is proportional to

$$L(t) \times p(t) \sim J\frac{p^2(t)}{p(t)+P_t(t)} \qquad (6)$$

After several hours of aging, the density of generated hole traps P_t will exceed the density of free holes ($P_t >> p$). In that case, equation (6) can be simplified to

$$L(t) \times p(t) \sim J\frac{p^2(t)}{P_t(t)} \qquad (7)$$

In a space-charge-limited PLED device the average density of free holes is proportional to the square root of current density ($p \sim J^{1/2}$), hence we have

$$L(t) \times p(t) \sim \frac{J^2}{P_t(t)} \qquad (8)$$

Substitution of equation (8) into equation (2) then gives

$$\frac{dP_t(t)}{dt} = \gamma \times L(t) \times p(t) \qquad (9)$$

Here γ is a proportionality constant for hole trap generation. This result indicates that the observed rate for hole trap formation can be explained by the interaction between

generated excitons and free holes. Furthermore, with the decrease of exciton and free hole densities due to hole trap formation during PLED degradation, the rate of trap formation also slows down. Using the experimentally determined rate of hole trap formation $dP_t(t)/dt$ combined with $L(t)$ and $p(t)$ from the numerical simulations we find that $\gamma=(5\pm2)\times10^{-27}$ cm^3.

The analysis presented above based on equations [5,6] consistently explains the experimental rate of hole trap formation (equation [2]), under the assumption that $P_t >> p$. The resulting rate then leads to a square-root dependence of the trap concentration with time that is proportional to the current density J. However, for an unaged PLED, the hole transport is trap free, so that at the start of the degradation experiment the density of hole traps is much smaller than the density of free holes ($P_t << p$). In that case, equation [5] simplifies to

$$L(t) \sim J \tag{10}$$

Consequently, the product of density of exciton generation rate and density of free holes becomes

$$L(t) \times p(t) \sim J \times p(t) \sim J^{\frac{3}{2}} \tag{11}$$

Following the same analysis this then would lead to a rate of hole trap formation of

$$\frac{dP_t(t)}{dt} \sim L(t) \times p(t) \sim J^{\frac{3}{2}} \tag{12}$$

Correspondingly, the time dependence of the hole trap concentration then becomes

$$P_t(t) = \beta \times J^{\frac{3}{2}} \times \mathrm{t} \tag{13}$$

As a result, assuming that interactions between free holes and excitons are responsible for the hole trap formation, we find that initially the amount of hole traps is expected to grow linearly with time, until the moment where the amount of hole traps exceeds the free hole density. Then the growth of traps slows down to a square-root dependence on time. As shown in Figures 2a and 5b experimentally indeed a linear increase of the hole trap concentration is observed at short times, represented by the blue lines with slope unity in the log P_t – log t plots. The initial fast increase of driving voltage and decrease of luminance in a PLED lifetime experiment was attributed to morphological changes,[2] here we show that it is a direct result of the

competition between free holes that enhance Langevin recombination and hole traps giving rise to non-radiative trap-assisted recombination,

In Figure 6a we zoom in on the hole trap formation in the first few hours. It is observed that the time period of the initial linear increase is shortened at higher currents. At higher currents, more hole traps are formed such that the condition that $p \approx P_t$ is reached earlier in time. Furthermore, equation 13 predicts that in the linear regime the hole trap concentration scales with $J^{3/2}$. In Figure 6b this dependence is confirmed, showing that the PLED degradation is governed by the formation of hole traps due to exciton-charge carrier (polaron) interactions at all times.

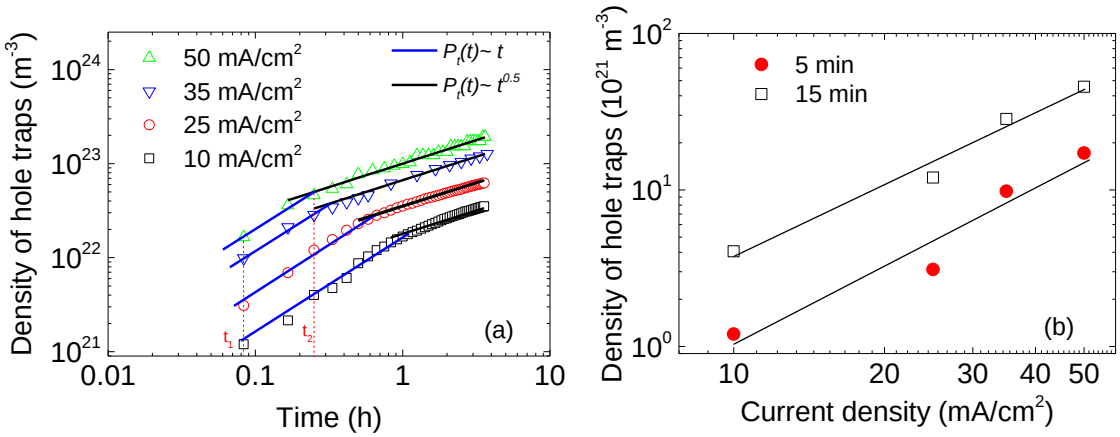

Figure 6. (a) Density of hole traps formed during degradation of SY-PPV PLEDs at four different current densities: 10, 25, 35, 50 mA/cm^2. Symbols are experimental data, black lines with slope 0.5 and blue lines with slope 1.0 are indicated as guide to the eye. (b) Density of hole traps under different aging current densities after a short period (t_1 = 5 min, t_2 = 15 min) of aging. Lines with a slope of 1.5 are indicated as a guide to the eye.

Until now, no distinction has been made whether the generated excitons have a singlet or triplet character. In a fluorescent PLED, 25% of the excitons formed by Langevin recombination exhibit the singlet spin state, whereas 75% are formed with the triplet spin state. Recombination of singlet excitons is fast: time-resolved photoluminescence measurement revealed a singlet exciton lifetime τ_S of 1.8 ns for SY-PPV at room

temperature. In contrast, the transition of the triplet state to the ground state is spin-forbidden and therefore very slow, the triplet exciton lifetime τ_T in PPV derivatives was previously reported to be around 100 µs. [16-18] This large difference in exciton lifetime strongly affects the steady-state concentration of singlet *[S]* and triplet *[T]* excitons in a PLED under operation, given by $[S]=0.25\times L\times\tau_S$ and $[T]=0.75\times L\times\tau_T$. As a consequence, the steady-state amount of triplet excitons in an operating PLED can be 4-5 orders of magnitude larger than the amount of singlet excitons. Furthermore, in an unaged operating PLED, the density of free electrons is much smaller than the density of free holes due to the present of electron traps.[19] Therefore, the interactions between triplet excitons (triplet-triplet annihilation) and between triplet excitons and free holes are expected to be dominant processes in an operating PLED. If the interaction between triplet excitons and free holes is the cause of hole trap formation, equation (9) can be rewritten as

$$\frac{dP_t(t)}{dt} = \gamma \times \frac{[T(t)]}{0.75\tau_T} \times p(t) = R_{T-p} \times [T(t)] \times p(t) \quad (14)$$

with $R_{T\text{-}p}$ a rate constant for hole trap formation due to interaction of a triplet exciton with a free hole. Using τ_T=100 µs and γ=5×10^{-27} cm^3, the rate constant $R_{T\text{-}p}$ amounts to (6.6±2) ×10^{-23} cm^3 s^{-1}. The interaction of triplet excitons and charge carriers (polarons) in a conjugated polyspirobifluorene polymer was previously investigated by Hertel et al., reporting a triplet-polaron recombination constant $k_{T\text{-}p}$ of (4 ± 1) ×10^{-13} cm^3 s^{-1}. [20] Assuming a similar rate constant in PPV derivatives would mean that of all triplet exciton-polaron interactions occurring in a PLED about only 1 out of 10^{10} events leads to the formation of a hole trap. A similar result was also obtained in phosphorescent small molecule based OLEDs.[10]

Upon the interaction between a triplet exciton and a free hole, the energy of the exciton is transferred to the hole, which is excited to a higher energetic state. The majority of excited hole polarons will relax to their ground state via rapid (~ps)

internal energy conversion[21], whereas approximately only 1 out of 10^{10} interactions will lead to breaking of a bond via direct dissociation, a pre-dissociation route or through a 'hot molecule' mechanism.[22] The dissociation products may act as hole traps themselves or further react with adjacent molecules to form hole traps.

3.5 Unification of PLED degradation

An important question is whether the degradation results obtained on SY-PPV can be used to understand or even predict the degradation of PLEDs based on other PPV-derivatives. In a recent study it was shown that the charge and energy transport in a series of PPV derivatives can be tuned by engineering of their side chains.[23] Poly[2,5-bis(2′-ethyl-hexyl)-1,4-phenylenevinylene] (BEH-PPV) has two symmetrical alkoxy chains which limit the configurational freedom of the individual chains, resulting in a decreased energetic disorder and higher mobility as compared to poly[2-methoxy-5-(2′-ethyl-hexyloxy)-1,4-phenylenevinylene] (MEH-PPV) and SY-PPV (for chemical structures see Suppl. Info., Figure S2). The hole mobility of BEH-PPV amounts to 3×10^{-9} m^2/Vs, as compared to 5×10^{-11} m^2/Vs for MEH-PPV and 3×10^{-12} m^2/Vs for SYPPV, respectively. As a result, in a BEH-PPV based PLED the steady-state hole density will be lower than in a MEH-PPV or SY-PPV PLED when driven at the same current density. Furthermore, it should be noted that the efficiency (light output/current) of a PLED is mobility independent, since both current and Langevin recombination linearly scale with the mobility.[1] Thus, at a given current the amount of excitons generated in BEH-PPV, MEH-PPV and SY-PPV based PLEDs will be equal. According to Equation 14, for equal exciton generation rate *L(t)* in the three PPV polymers the higher steady-state hole density *p(t)* in SY-PPV is then expected to accelerate the hole trap formation. In contrast, BEH-PPV should be the most stable PLED with lowest trap generation rate, due to its higher mobility and resulting lower *p(t)*. In Figure 7a, the formation of hole traps is shown for the various PPV-based PLEDs, driven at a current density of 35 mA/cm^2. It is observed that the

hole trap formation is highest in SY-PPV and lowest in BEH-PPV. Subsequently, following Equation 14, in Figure 7b the hole trap formation is normalized to the (average) free hole density in the various PLEDs. Remarkably, the hole trap formation is now unified on one single curve.

This unification has two important consequences; first, it shows that radiative singlet excitons are not responsible for the degradation, it is only the steady-state hole concentration that matters. As stated above, the generation rate for singlet and triplet excitons via Langevin recombination is independent on mobility. However, by lowering the charge carrier mobility with bulky asymmetric side-chains, as in SY-PPV, also the singlet exciton diffusion is slowed down.[23] This slower exciton diffusion in SY-PPV as compared to BEH-PPV reduces the quenching of singlet excitons at defects, leading to longer photoluminescence (PL) decays (~0.2 ns for BEH-PPV, ~1.8 ns for SY-PPV) and higher PL efficiency (~40% for SY-PPV, ~7% for BEH-PPV). So although the formation rate of singlet and triplet excitons in SY-PPV and BEH-PPV PLEDs is equal, the amount of photons emitted in a SY-PPV PLED is higher due to the higher PL quantum yield. When these radiative singlet excitons would be responsible for degradation, a unification based only on steady-state hole density would not be possible. Second, the name 'super' yellow PPV originates from the fact that it was considered as the first polymer with sufficient stability for certain PLED applications. It was believed that its bulky side-chain provided a steric protection of the vulnerable vinyl bonds. However, our results (Figure 7a) show that this was a misconception. The bulky side-chain increases the energetic disorder, lowers the mobility and exciton diffusion and increases the PL efficiency. Furthermore, the color shift towards yellow (as compared to the orange emitting MEH-PPV and BEH-PPV) also leads to an increase in the measured luminance (cd/m^2). Since lifetime testing on PLEDs was done at equal luminance and not at equal current density the SY-PPV PLEDs were simply stressed at lower currents as compared to other PPV derivatives. This compensated for the increased steady-state hole density and therefore SY-PPV PLEDs seemed more stable.

The now obtained insight in PLED degradation provides options for further

improvement of their operational lifetime. Reuced hole trap formation is obtained by a combination of an increased charge carrier mobility and a decrease of the triplet lifetime. Another important question is how the rate constant for hole trap formation $R_{T\text{-}p}$ depends on the chemical structure of the polymer. Both issues will be addressed in future studies and will boost the applicability of PLEDs.

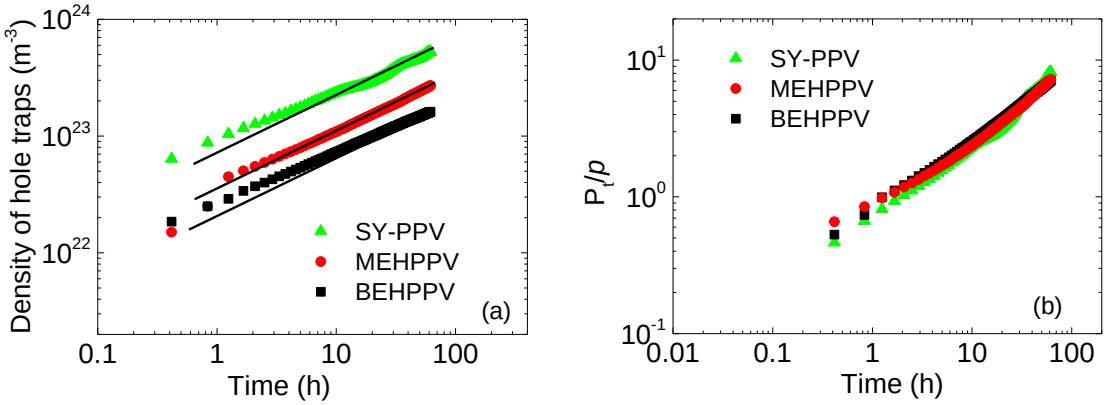

Figure 7. (a) Density of hole traps formed during degradation of SY-PPV, BEHPPV, and MEHPPV PLEDs at an aging current density of 35 mA/cm^2. Symbols are experimental data, black lines with slope 0.5 are indicated as guide to the eye. (b) Density of hole traps formed during degradation normalized on the average density of free holes during aging.

3.6 Conclusion

In conclusion, by evaluation of the voltage drift of a PLED upon aging, the density of hole traps as function of aging time has been calculated. With the amount of hole traps known, the luminance decay of the PLED could be predicted. The agreement with experiment demonstrates that the decrease of the radiative recombination under stress is a direct consequence of increased non-radiative recombination of trapped holes with free electrons. It has been found that initially the density of hole traps increases linearly with time, and after a short stress period the trap formation is

slowed down to a square root dependence on time. The observed hole trap generation could be linked to the product of exciton density and density of free holes. Hole trap formation due to the interaction between triplet excitons and free holes (polarons) enables unification of the degradation of various PPV derivatives.

Supplementary Information

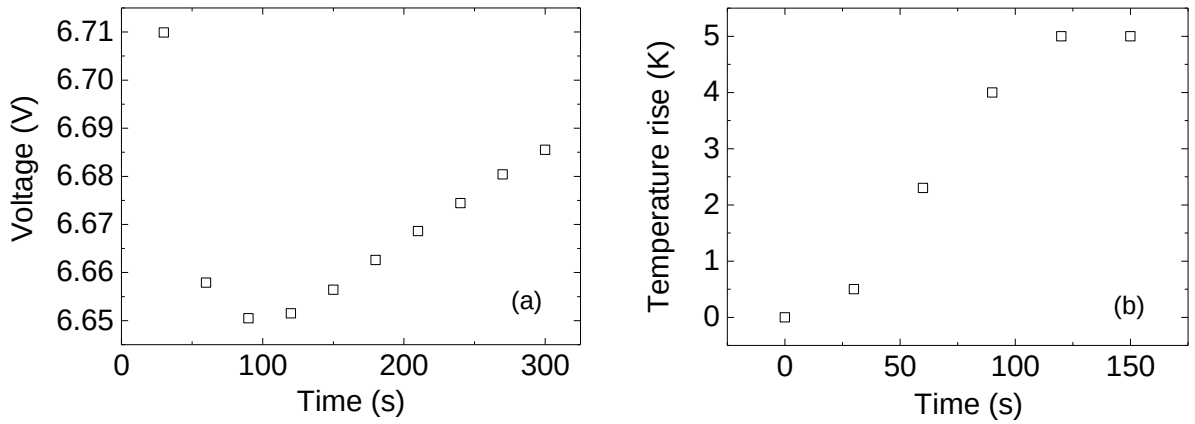

Figure S1. (a) Driving voltage of a SY-PPV PLED aged at 50 mA/cm^2 in the first 5 minutes; the thickness of the SY-PPV layer is 100 nm. (b) Modelled temperature rise with stressing time of a SY-PPV PLED aged at 50 mA/cm^2.

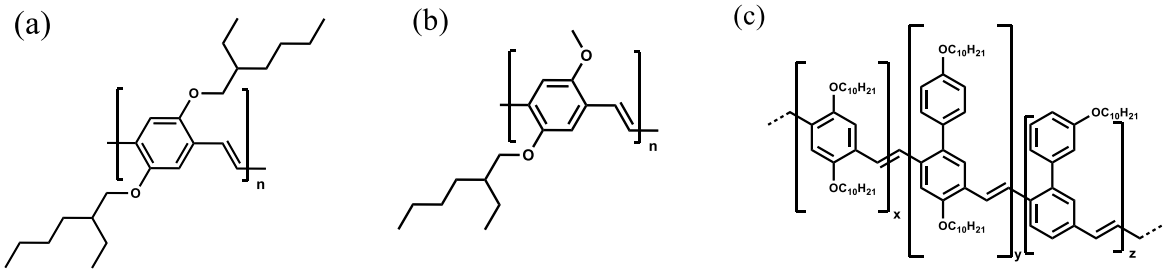

Figure S2. Chemical structures of (a) BEH-PPV, (b) MEH-PPV and (c) SY-PPV.

References

[1] Q. Niu, G. J. A. Wetzelaer, P. W. Blom, N. I. Crăciun. *Advanced Electronic Materials* **2016**, *2*.

[2] M. Kuik, G. J. A. Wetzelaer, H. T. Nicolai, N. I. Craciun, D. M. De Leeuw, P. W. Blom, *Advanced Materials* **2014**, *26*, 512.

[3] W. Shockley, W. T. Read. *Physical Review* **1952**, *87*, 835.

[4] T. Yoshioka, K. Sugimoto, K. Katagi, Y. Kitago, M. Tajima, S. Miyaguchi, T. Tsutsui, R. Iwasaki, Y. Furukawa, *SID Symposium Digest of Technical Papers* **2014**, *45*, 642.

[5] L. Yang, B. Wei, J. Zhang. *Semiconductor Science and Technology* **2012**, *27*, 105011.

[6] M. Mandoc, B. de Boer, G. Paasch, P. Blom. *Physical Review B* **2007**, *75*, 193202.

[7] H. Nicolai, M. Mandoc, P. Blom. *Physical Review B* **2011**, *83*, 195204.

[8] C. Tanase, P. W. M. Blom, D. M. de Leeuw. *Physical Review B* **2004**, *70*, 193202.

[9] I. D. Parker, Y. Cao, C. Y. Yang. *Journal of Applied Physics* **1999**, *85*, 2441.

[10] N. C. Giebink, B. W. D'Andrade, M. S. Weaver, P. B. Mackenzie, J. J. Brown, M. E. Thompson, S. R. Forrest. *Journal of Applied Physics* **2008**, *103*, 044509.

[11] S. Scholz, D. Kondakov, B. Lüssem, K. Leo. *Chemical Reviews* **2015**, *115*, 8449.

[12] T. D. Schmidt, L. Jäger, Y. Noguchi, H. Ishii, W. Brütting. *Journal of Applied Physics* **2015**, *117*, 215502.

[13] G. C. M. Silvestre, M. T. Johnson, A. Giraldo, J. M. Shannon. *Applied Physics Letters* **2001**, *78*, 1619.

[14] P. Langevin. *Ann. Chim. Phys* **1903**, *28*, 443.

[15] M. Kuik, L. Koster, G. Wetzelaer, P. Blom. *Physical review letters* **2011**, *107*, 256805.

[16] A. S. Dhoot, D. S. Ginger, D. Beljonne, Z. Shuai, N. C. Greenham. *Chemical Physics Letters* **2002**, *360*, 195.

[17] R. D. Scurlock, B. Wang, P. R. Ogilby, J. R. Sheats, R. L. Clough. *Journal of the American Chemical Society* **1995**, *117*, 10194.

[18] H. D. Burrows, J. S. de Melo, C. Serpa, L. Arnaut, M. d. G. Miguel, A. Monkman, I. Hamblett, S. Navaratnam. *Chemical physics* **2002**, *285*, 3.

[19] H. T. Nicolai, M. Kuik, G. Wetzelaer, B. De Boer, C. Campbell, C. Risko, J. Brédas, P. Blom. *Nature materials* **2012**, *11*, 882.

[20] D. Hertel, K. Meerholz. *The Journal of Physical Chemistry B* **2007**, *111*, 12075.

[21] W. Wild, A. Seilmeier, N. H. Gottfried, W. Kaiser. *Chemical Physics Letters* **1985**, *119*, 259.

[22] N. Nakashima, K. Yoshihara. *The Journal of Physical Chemistry* **1989**, *93*, 7763.

[23] I. Rörich, O. V. Mikhnenko, D. Gehrig, P. W. M. Blom, N. I. Crăciun. *The Journal of Physical Chemistry B* **2017**, *121*, 1405.

Chapter 4 Origin of negative capacitance in bipolar organic diodes

In this chapter, the information of hole trap formation during PLED degradation is used to understand the origin of negative differential capacitance (NC) observed at low frequencies in PPV based PLEDs. We study the origin of the NC effect by systematically varying the amount of electron and hole traps in the polymeric semiconductor. Increasing the electron and hole trap density enhances the NC effect. The magnitude and observed decrease of the relaxation time is consistent with the (inverse) rate of trap-assisted recombination. The absence of NC in a nearly trap-free PLED unambiguously shows that trap-assisted recombination is the responsible mechanism for the negative contribution to the capacitance in bipolar organic diodes.

4.1 Introduction

Impedance spectroscopy is a powerful technique to study charge transport and recombination in semiconductors, since it enables to differentiate between processes that are relevant on different timescales [1]. In organic LEDs, where electrons and holes are simultaneously injected, a negative contribution to the differential capacitance C has been observed at low frequencies [2-6]. For an applied voltage just above the built-in voltage V_{bi} the differential capacitance can even become negative. Several explanations have been proposed, including bimolecular recombination [2], electron injection through interfacial states [3], accumulation of charges at an organic/organic interface [4], trap-assisted monomolecular recombination [5,6], self-heating [7], and energetic disorder [8]. The concept of a negative capacitance in semiconducting devices was discussed by Ershov et al. [9]. Recombination of electrons and holes results in a recombination current j_r. The negative contribution to the capacitance (NC) can be related to a time domain response on a voltage step ΔV. A positive derivative of the transient recombination current dj_r/dt will result in a negative contribution to the capacitance [9]. For a single exponential transient, given by $j_r(t)=-j_0\exp(-t/\tau_r)$, with j_0 the prefactor of the recombination current j_r, the capacitance is given by

$$C(\omega) = C_0 - \frac{C_1}{1+\omega^2\tau_r^2} \qquad (1)$$

with C_0 the geometrical capacitance $\varepsilon_0\varepsilon_r A/d$, ω the angular frequency, C_1 a proportionality factor given by $j_0\tau_r/\Delta V$ and τ_r the relaxation time [9]. In an early study by Ehrenfreund et al. [5], Eq. (1) was used to fit the frequency dependence of the capacitance $C(\omega)$ at various voltages. A relaxation time τ_r of 0.5 ms was fitted, whereas the proportionality factor C_1 was not quantified. The fact that at low frequencies $C(\omega)$ could be described by a voltage independent τ_r was then considered as an indication for trap-assisted recombination. It was argued that for bimolecular recombination τ_r should decrease with voltage due the increasing carrier density. However, the magnitude of τ_r was not further explained. In a later study by Djidjou et

al. [6], a similar approach was followed; to describe $C(\omega)$ they found $C_1(V)$ to be exponentially dependent on voltage, combined with a frequency independent τ_r. However, the functional dependence of $C_1(V)$ and the magnitude of τ_r were not quantitatively addressed.

In the last two decades, effort has been dedicated to the understanding of the physical processes that govern PLED device operation. These processes include injection, transport, and recombination (radiative and non-radiative) of charge carriers. The hole transport in many conjugated polymers exhibits trap-free behavior, whereas the electron transport is strongly limited by traps [10]. For a range of conjugated polymers, these electron traps were observed to be situated at an energy of ~3.6 eV below the vacuum level with a typical density of ~10^{23} m^{-3}. The electron traps not only limit the electron transport, but the trapped electrons also recombine with free holes via a nonradiative trap-assisted recombination process, which competes with the emissive bimolecular Langevin recombination [10]. For trap-assisted recombination of free holes with trapped electrons in a PLED the relaxation time τ_r is given by

$$\tau_r = \frac{1}{N_t C_p} \qquad (2)$$

with N_t the electron trap concentration and C_p the hole capture coefficient, given by $(q/\varepsilon_0\varepsilon_r)\mu_p$, with μ_p the hole mobility [10]. Thus, for a quantitative analysis of a relaxation time τ_r resulting from trap-assisted recombination knowledge of the amount of traps and capture coefficient (charge carrier mobility) is required.

A more direct proof for whether charge traps are involved in the negative contribution to the capacitance, as compared to the voltage independence of τ_r, would be a direct variation of the relaxation time τ_r by changing the amount of traps N_t. In the present study we systematically vary the amount of traps in PLEDs based on poly(p-phenylene vinylene) derivatives. An increase of the negative contribution to the capacitance is observed by increasing the amount of electron traps by addition of a fullerene based electron acceptor. Upon degradation under current stress hole traps are formed in a PLED [11], which also give rise to an enhanced NC. The observed changes in relaxation time are quantitatively in correspondence with trap-assisted

recombination. In contrast, trapping effects can be strongly suppressed by blending the semiconductor with a large band gap host [12]. This trap dilution nearly eliminates the negative contribution to the capacitance, unambiguously proving that recombination via traps is responsible for the negative capacitance observed in PLEDs.

4.2 Experiment

In the present study organic bipolar diodes were prepared using a poly(p-phenylene vinylene) (PPV) based copolymer, known as 'super yellow' (SY-PPV, Merck AG) [13]. The SY-PPV was dissolved in toluene and subsequently spin-coated onto a glass/ITO/PEDOT:PSS substrate. Cathode materials were then thermally evaporated on top of the polymer (chamber pressure 10^{-7} mbar). The corresponding device architecture of the PLED is ITO/PEDOT/Polymer/Ba (5 nm)/Al (100 nm). To increase the amount of electron traps phenyl-C61-butyric acid methyl ester (PCBM) with a LUMO level of -3.7 eV, which lies well below the LUMO of SY-PPV (~3.0 eV), was dissolved in chlorobenzene and added to the polymer solution. The solution was then stirred overnight for device preparation. In the aging test, a SY-PPV PLED was stressed under a constant current density of 10 mA/cm^2 and impedance measurements were performed as a function of aging time. The impedance data were taken using an Agilent 4284a RCL meter, with the DC bias swept from -2 V to 5 V, superposed by an AC bias of 100 mV at various frequencies *f*. All devices were fabricated and measured under inert N_2 atmosphere. For PLEDs based on a polymer blend poly[2-methoxy-5-(2-ethylhexyloxy)-1,4-phenylenevinylene] (MEH-PPV) was mixed with poly(vinylcarbazole) (PVK) in various ratios and dissolved in chlorobenzene.

4.3 Negative contribution to the PLED capacitance

As first step we carry out impedance measurements on a pristine SY-PPV based PLED. We note that in earlier studies the electron and hole transport of SY-PPV has been well characterized. Using the electron and hole transport data also the

current and light-output of the bipolar PLED were consistently modelled [11]. The *C-V* characteristics of a pristine SY-PPV PLED at various frequencies are shown in Figure 1.

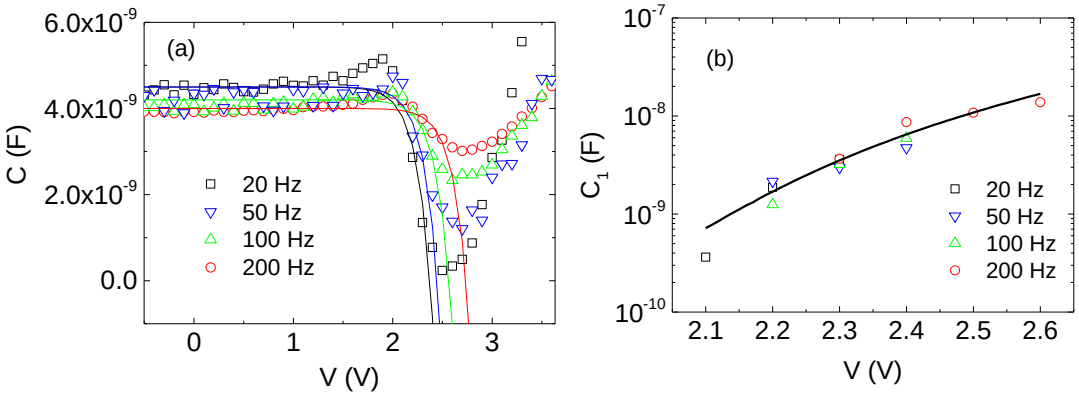

Figure 1. (a) *C-V* characteristics of a SY-PPV PLED at different frequencies. The empty symbols represent the experimental data for an active layer thickness of 120 nm, while the solid lines are a fit to Eq. (1). (b) $C_1(V)$ values obtained from Eq. (1) at various frequencies (empty symbols). For comparison also the normalized *J-V* characteristic (line) of a SY-PPV PLED in the voltage range where the NC effect is dominant is shown.

At negative bias, the PLED is fully depleted and the capacitance equals C_0, the geometric capacitance of the device. At a low frequency of 20 Hz, the capacitance first slightly increases with voltage, reaching a maximum value close to the built-in voltage (V_{bi}) of the PLED. This maximum in the capacitance originates from hole accumulation at the polymer/anode interface as a result of hole diffusion to establish Fermi-level alignment [14]. At higher frequencies the peak capacitance decreases. After the peak value, the negative contribution to the capacitance sets in, and the capacitance decreases with voltage until it reaches a minimum of only 0.2 nF at 2.5V. As the frequency increases the decrease of capacitance becomes weaker. By applying Eq. (1) with τ_r and C_1 as fitting parameters, the decrease of the capacitance as a function of voltage at various frequencies is fitted, as shown in Figure 1 (a) (solid

lines). We obtain a voltage independent relaxation time τ_r of 2.5±0.5 ms for the SY-PPV based PLED. We note that the negative effect on the capacitance only occurs in a limited voltage range. At higher voltages the amount of injected charges strongly increases and charge accumulation regions close to the electrodes are formed, leading again to an increase of the capacitance (the electrodes 'grow' into the active polymer layer). The obtained τ_r of 2.5 ms is close to the relaxation time of 0.5 ms as reported earlier for MDMO-PPV [5]. Furthermore, we also obtain the voltage dependence of C_1, as shown in Figure 1b. Similar to Djidjou et al. [6], a steep increase of C_1 with voltage is found. From modeling of SY-PPV based hole- and electron only devices the hole mobility $\mu_p=3\times10^{-12}$ m^2/Vs and electron trap density $N_t=1\times10^{23}$ m^{-3} have been determined [11]. Using a relative dielectric constant $\varepsilon_r=3$ the capture coefficient for a trapped electron to capture a free hole, given by $C_p= q\mu_p/\varepsilon_r\varepsilon_0$, amounts to 1.8×10^{-20} m^3 s^{-1}. The relaxation time $\tau_r = (N_tC_p)^{-1}$ then equals 0.6 ms. The experimentally obtained relaxation time τ_r of 2.5 ms is slightly larger than the estimated value of 0.6 ms for trap-assisted recombination. The proportionality factor $C_1(V)$ is linearly dependent on the recombination current j_r. In a PLED at low voltages the total recombination is per definition proportional to the current density J. As a result, the voltage dependence of j_0, and therefore C_1, should be identical to the voltage dependence of J. In Figure 1b the normalized PLED current density J is compared with $C_1(V)$. It is shown that indeed their voltage dependence is identical. Furthermore, $C_1(V)$ is frequency independent. The near-exponential dependence of $C_1(V)$ is therefore the result of the density- and field dependent charge carrier mobility in the space-charge limited PLED. Thus, we find that the NC behavior of a pristine SY-PPV PLED can be described by a voltage-independent relaxation time that is close to the expected value for trap-assisted recombination. The voltage dependence of the pre-factor C_1 is governed by the PLED current that originates from the density- and field dependence of the charge carrier mobility. To further investigate whether the NC is indeed a trap-assisted recombination induced phenomenon, we vary the amount of electron and hole traps in SY-PPV and determine the dependence of τ_r and $C_1(V)$ on trap density.

Electron traps are added by blending SY-PPV with fullerene based PCBM

molecules of which the lowest unoccupied molecular orbital (LUMO) at ~3.8 eV is far below the LUMO of SY-PPV (~3.0 eV). PCBM is incorporated into SY-PPV with concentrations of 0.010% 0.024% and 0.050% (wt). These concentrations corresponds to additional electron trap densities of 2×10^{23} m^{-3}, 4.6×10^{23} m^{-3} and 1×10^{24} m^{-3}, respectively. The *C-V* characteristics (f=20 Hz) of the pristine SY-PPV PLED and the devices with various PCBM concentrations are shown in Figure 2. By increasing the amount of electron traps the negative contribution to the capacitance becomes more pronounced and shifts to higher voltages. For the pristine SY-PPV PLED, with an electron trap concentration N_{t0} of 1×10^{23} m^{-3}, first $C_1(V)$ and relaxation time τ_0 are determined from the frequency response, similar as discussed above. For the analysis of the PLEDs with additional electron traps we assume the relaxation time to vary according to $\tau_r = \tau_0(N_{t0}/N_{tot})$, with $N_{tot} = N_{t0} + N_{tPCBM}$. Using these relaxation times we then fit $C_1(V)$ for the PLEDs with various amount of electron trap concentrations N_{tot}, the result is shown in Figure 3a. For trap-assisted recombination the proportionality factor C_1 is equal to $C_1=j_0\tau_r/\Delta V$ [9]. We note that j_0 is nearly independent on the amount of electron traps, since the PLED current is hole dominated. With $\tau_r = \tau_0(N_{t0}/N_{tot})$ the factor $C_1(N_{tot}/N_{t0})$ should then be independent on the electron trap concentration. In Figure 3b the normalized factor $C_1(N_{tot}/N_{t0})$ is shown as a function of voltage for the various electron trap concentrations. As expected for trap-assisted recombination this normalization unifies the prefactor C_1 and gives a unique relation for $C_1(N_{tot}/N_{t0})$ (V). Together with $\tau_r = \tau_0(N_{t0}/N_{tot})$ from Eq. (1) the negative contribution NC of the capacitance for the PLEDs with additional traps can then be predicted from the pristine device (τ_0, N_{t0}). As shown in Figure 2 the measured *C-V* characteristics (symbols) match well with the predicted values (lines) for every electron trap concentration. Thus, the NC effect changes with electron trap concentration as expected for trap-assisted recombination being the dominant relaxation mechanism.

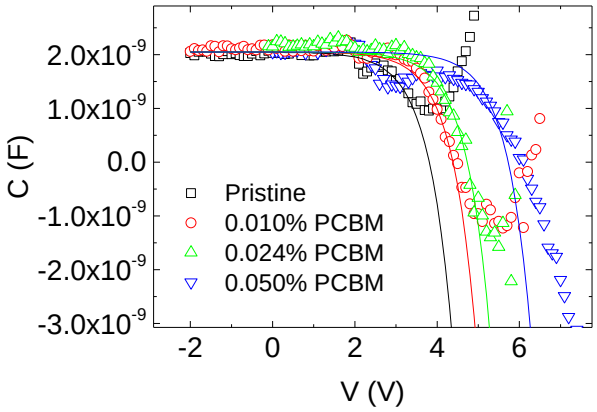

Figure 2. Experimental *C-V* characteristics (symbols) at *f*=20 Hz of a pristine SY-PPV based PLED and SY-PPV PLEDs with additional PCBM electron traps, with concentrations of 0.010%, 0.024% and 0.050% (wt), respectively. The active layer thickness of the PLEDs amounts to 150 nm. The solid lines are calculated using Eq. (1).

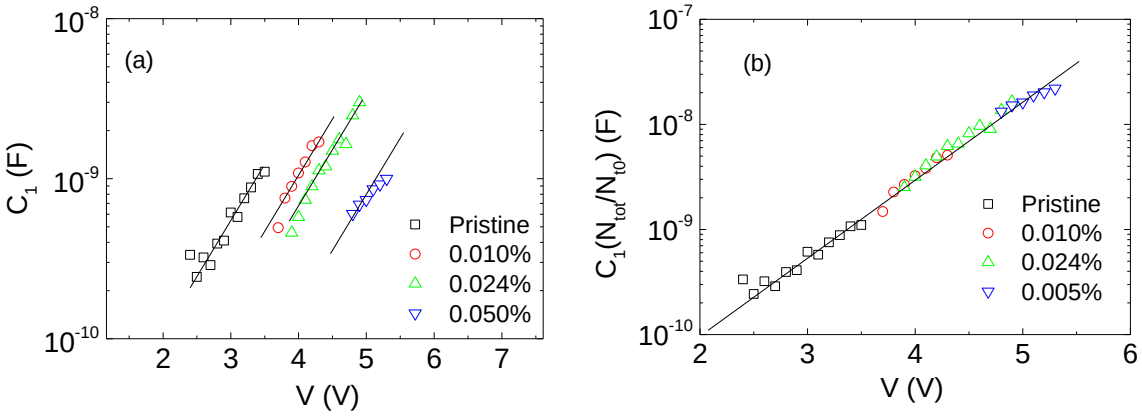

Figure 3. (a) C_1 as a function of voltage V for a pristine SY-PPV PLED and SY-PPV PLEDs with additional electron traps (PCBM). The total amount of electron traps N_{tot} ranges from 1×10^{23} m^{-3} for the pristine device (N_{t0}) to 3×10^{23} m^{-3}, 5.6×10^{23} m^{-3} and 1.1×10^{24} m^{-3} for the PLEDs with PCBM concentrations of 0.010%, 0.024% and 0.050% (wt), respectively. (b) Normalized proportionality factor $C_1(N_{tot}/N_{t0})$ (V). The active layer thickness of the PLEDs amounts to150 nm.

4.4 Negative capacitance during PLED degradation

In an earlier study it has been demonstrated that during current stress hole traps are

formed in PLEDs. The number of hole traps can be determined by modelling the current density-voltage (*J-V)* and light-output-voltage characteristics of a degraded device [11]. As a result, by varying the aging time different amount of hole traps can be created in PLEDs under current stress. This enables us to address the effect of hole traps on the negative capacitance effect. For this purpose, SY-PPV based PLEDs were aged under a constant current density of 10 mA/cm^2 for 3 hours, 17 hours and 56 hours, respectively. The corresponding densities of generated hole traps then amount to 4.6×10^{22} m^{-3} (3 hours), 1.1×10^{23} m^{-3} (17 hours) and 2.0×10^{23} m^{-3} (56 hours). The *C-V* characteristics measured at 100 Hz of the devices are shown in Figure 4a. It is observed that, similar to the increasing density of electron traps (Figure 2), the negative capacitance effect gets more pronounced with aging and shifts to higher voltages. The generated hole traps lead to additional trap-assisted recombination of free electrons with trapped holes. Since in PPV derivatives the mobility of free electrons and holes are equal [10], also the capture coefficients C_n and C_p are equal. As a result, the relaxation time for recombination of free holes with trapped electrons (Eq. (2) has a similar prefactor as the recombination of free electrons with trapped holes, so that both contributions can be simply added. The relaxation time is then governed by the total amount of traps $N_{tot}=N_{t0}+P_t$, with $N_{t0}=1\times10^{23}$ m^{-3} the density of electron traps in a pristine device and P_t the amount of hole traps generated during degradation. A complication with regard to the analysis presented before for the PCBM electron traps is that the generation of hole traps lowers the hole dominated current of the PLED. Consequently, the recombination current j_0 and therefore $C_1(N_{tot}/N_{t0})$ will also depend on the hole trap concentration. However, in Figure 1b we have demonstrated that j_0 scales with the PLED current density J. In Figure 4b, using $\tau_r= \tau_0(N_{t0}/N_{tot})$, the fitted $C_1(N_{tot}/N_{t0})$ is shown as a function of voltage, together with the normalized experimental *J-V* characteristics of the degraded devices. As expected, the obtained $C_1(N_{tot}/N_{t0})$ scales with the PLED current density J. Since it is known how J varies with P_t, also the dependence of both j_0 and $C_1(N_{tot}/N_{t0})$ (V) on hole trap density is known. The *C-V* characteristics of the degraded PLEDs can then be predicted from the pristine device using Eq. (1) in combination with $\tau_r= \tau_0(N_{t0}/N_{tot})$. The calculated

negative contributions to the *C-V* characteristics are shown in Figure 4a and agree well with the experimental data. This demonstrates that recombination of free electrons and trapped holes after degradation also contributes to the NC effect, and their contribution can be added to the recombination of free holes with trapped electrons in pristine PLEDs. The quantitative agreement also shows that impedance spectroscopy can be used as a tool to study degradation in organic devices to determine trap densities from the observed relaxation times.

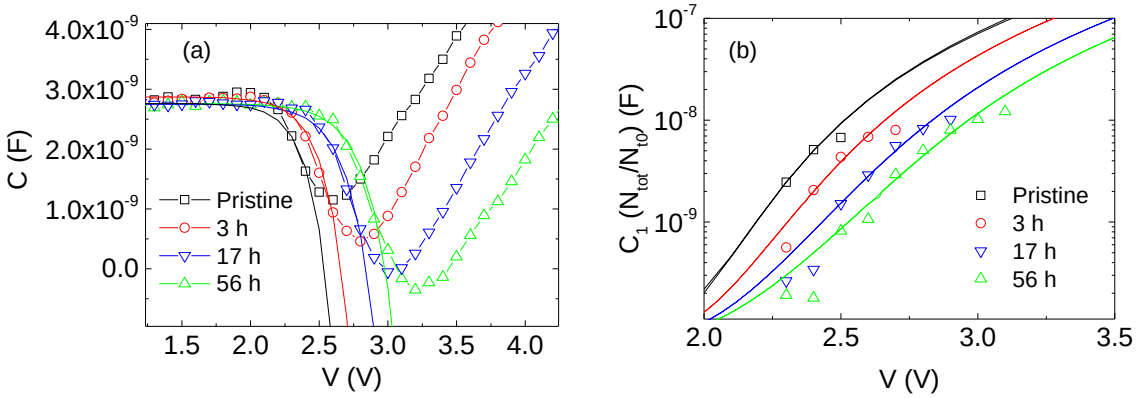

Figure 4. (a) Measured *C-V* characteristics (symbols) (*f*=100 Hz) of a pristine SY-PPV PLED and PLEDs stressed at a constant current of 10 mA/cm^2 for different aging periods. The PLED active layer thickness amounts to 100 nm. The solid lines are calculated using Eq. (1) with $\tau_r = \tau_0(N_{t0}/N_{tot})$. (b) Voltage dependence of proportionality factor $C_1(N_{tot}/N_{t0})$ and normalized experimental current densities of pristine and aged SY-PPV PLEDs.

4.5 Elimination of negative contribution in blend PLEDs

A final and unambiguous proof for the role of trap-assisted recombination to the negative contribution in the capacitance would be the absence of the NC effect in a PLED without traps. It has recently been shown that the effect of trapping in semiconducting polymers can be strongly suppressed by blending the active polymer with a large bandgap host [12]. The trap dilution effect strongly enhances the trap-limited electron current and simultaneously leads to a reduction of the

trap-assisted recombination. It is therefore expected that, in case trap-assisted recombination is responsible for the NC effect, dilution of traps will suppress this negative contribution to the capacitance. To study the effect of trap dilution on the capacitance at low frequencies we blend MEH-PPV (semiconductor) with PVK (host) using MEH-PPV: PVK blend ratios of 1:0 (pristine MEH-PPV), 1:1 and 1:3 (wt), respectively. The *C-V* characteristics of the corresponding blend PLEDs at *f*=20 Hz are shown in Figure 5. In a 1:3 blend PLED, where electron trapping is strongly suppressed [12], the negative contribution to the capacitance is completely eliminated. After the shallow maximum in the capacitance due to hole accumulation at the anode the capacitance does not drop below its geometrical value C_0. This once more confirms that trap-assisted recombination is the true and only origin of the negative capacitance as observed in bipolar organic devices.

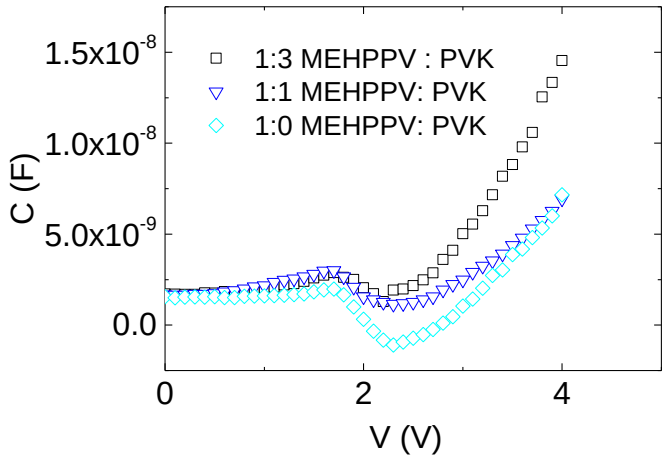

Figure 5. *C-V* characteristics at *f*=20 Hz of a pristine MEH-PPV PLED (1:0) and PLEDs consisting of MEH-PPV:PVK blends in ratios of 1:1 and 1:3, respectively. The thickness of pristine and blend polymer layer is 200 nm.

4.6 Conclusion

In conclusion, the negative contribution to the capacitance observed in the low frequency *C-V* characteristics of bipolar PLEDs is characterized by a voltage

independent relaxation time that is in the same order of magnitude as the inverse rate for trap-assisted recombination. Enhancement of the amount of electron traps by the addition of fullerene molecules leads to a more pronounced NC effect, which can be quantitatively explained by trap-assisted recombination. Furthermore, the enhanced NC effect in degraded PLEDs, in which hole traps are generated by current stress, can be attributed to trap-assisted recombination of free electrons with trapped holes. The absence of NC in a nearly trap-free PLED unambiguously shows that trap-assisted recombination is the only mechanism responsible for the negative contribution to the capacitance in bipolar organic diodes.

.

Reference

[1] J. R. MacDonald, *Impedance Spectroscopy* (John Wiley and Sons, New York, 1987) Chap. 1, p. 2.

[2] H. H. P. Gommans, M. Kemerink, and R. A. J. Janssen, Phys. Rev. B **72**, 235204 (2005).

[3] J. Bisquert, G. Garcia-Belmonte, A. Pitarch, and H. J. Bolink, Chem. Phys, Lett. **422**, 184 (2006).

[4] L. S. C. Pingree, M. T. Russell, T. J. Marks, and M. C. Hersam, J. Appl. Phys. **100**,044502 (2006).

[5] E. Ehrenfreud, C. Lungenschmied, G. Dennler, H. Neugebauer, and N. S. Sariciftci, Appl. Phys. Lett. **91**, 012112 (2007).

[6] T. K. Djidjou, T. Basel, and A. Rogachev, J. Appl. Phys. **112**, 024511 (2012).

[7] E. Knapp and B. Ruhstaller, J. Appl. Phys. **117**, 135501 (2015).

[8] W. C. Germs, S. L. M. van Mensfoort, R. J. de Vries, and R. Coehoorn, J. Appl. Phys. **111**, 074506 (2012).

[9] M. Ershov, H. C. Liu, L. Li, M. Buchanan, Z. R. Wasilewski, and A. K. Jonscher, IEEE Trans. Electron Devices ED-**45**, 2196 (1998).

[10] M. Kuik, G.-J. A. H. Wetzelaer, H.T. Nicolai, N.I. Craciun, D.M. De Leeuw, and P.W.M. Blom, Adv. Mater. **26**, 512 (2014).

[11] Q. Niu, G. A. H. Wetzelaer, P. W. M. Blom, N. I. Crăciun. Advanced Electronic Materials 1600103 2016).

[12] D. Abbaszadeh, A. Kunz, G. A. H.Wetzelaer, J. J. Michels, N. I. Crăciun, K. Koynov, I. Lieberwirth and P.W. M. Blom, Nature Materials **4626**, 628-633 (2016).

[13] H. Spreitzer, H. Becker, E. Kluge, W. Kreuder, H. Schenk, R. Demandt, H. Schoo, Advanced Materials **10**, 1340 (1998).

[14] S. L. M. van Mensfoort, R. Coehoorn, Phys. Rev. Lett. **100**, 086802 (2008).

Chapter 5 Transient electroluminescence on pristine and degraded phosphorescent blue OLEDs

In state-of-the-art blue phosphorescent organic light-emitting diode (PHOLED) device architectures electrons and holes are injected into the emissive layer, where they are carried by the emitting and hole transporting units, respectively. Using transient electroluminescence measurements, we disentangle the contribution of the electrons and holes on the transport and efficiency of both pristine and degraded PHOLEDs. By varying the concentration of hole transporting units we show that for pristine PHOLEDs the transport is electron dominated. Furthermore, degradation of the PHOLEDs upon electrical aging is not related to the hole transport, but is governed by a decrease of the electron transport due to the formation of electron traps.

5.1 Introduction

As discussed in Chapter 1, phosphorescent organic light-emitting diodes (OLEDs) always have complicated structures, which make it difficult to reveal the mechanisms behind device degradation. In this chapter, we apply transient electroluminescence (TEL) to pristine and degraded multi-layer PHOLEDs.[1] Using TEL measurements we can disentangle the electron and hole transport in these multi-layer structures, enabling us to directly trace the change of unipolar charge transport in the OLEDs before and after aging, We find that the degradation does not have an impact on the hole transport of the PHOLEDs, whereas for degraded PHOLEDs a decrease of the electron transport due to the generation of electron traps is detected.

5.2 Experiment

As a blue phosphorescent emitter a complex based on cyclometallated N-heterocyclic carbene (NHC) and iridium (BASF SE) is utilized to give blue-emitting PHOLEDs. This emitter has a longer lifetime (*LT70*=350 h for initial luminance L_0=1000 cd/m^2) than the commonly known blue phosphors like FIrpic[2,3] and iridium(III) bis(4′,6′-difluorophenylpyridinato)tetrakis(1-pyrazolyl)borate (FIr6)[4]. In the OLED device architecture used the emitting layer consists of the phosphorescent NHC dye (typically 10%) that is incorporated in a wide band gap matrix (85%) and is co-doped with a high band gap hole transport molecule (5%) in order to fine-tune charge balance and to reduce hole-exciton interactions on the emitter which is transporting the electrons. The energy band diagram of the device is schematically shown in Figure 1a, where ionization potentials (IP, often termed “HOMO”) have been obtained by UPS measurements. As adding optical gaps to those values to estimate electron affinities (EA, often termed “LUMO”) can lead to large errors due to the electron-hole interaction, we have calculated electron affinities by density functional theory (DFT).

To this end neutral and charged molecules were geometry optimized in the gas phase using the generalized gradient approximation functional of Becke[5] and Perdew (BP86) [6] in combination with polarized double-ζ valence (def2-SVP) basis sets as implemented in the TURBOMOLE program package.[7] Energy differences between neutral and charged states were then evaluated on the optimized structures with the same functional but a polarized triple-ζ valence (def2-TZVP) basis within the conductor-like screening model (COSMO),[8] that considers the organic solid-state environment simply by assuming a dielectric continuum of relative permittivity ε_r = 4.5. Note that we have also calculated the IP accordingly and find reasonable agreement with the UPS measurements (+-0.1eV for all molecules) except for the organic host. There the deviation is stronger due to a localization problem in the DFT calculation originating from the molecular symmetry with respect to the hole-transporting moieties. This problem does not occur in case of the EA calculation due to the different symmetry with respect to electron transporting moieties in the organic host.

Charge transport and recombination in the emission layer is explained in Figure 1b, while Figure 1c depicts the OLED stack which is prepared in the following way: on top of a glass/ITO substrate a 80 nm film of tris[(3-phenyl-1H-benzimidazol-1-yl-2(3H)-ylidene) -1,2-phenylene]-iridium (DPBIC) p-doped with 10% molybdenum(VI) oxide was evaporated as hole transport layer (HTL). Subsequently, a 10 nm undoped layer of DPBIC (hole mobility of 1.6×10^{-5} cm^2/Vs at a field of 1.0×10^6 V/cm.[9]) was then deposited as exciton and electron blocking layer (EBL) due to its extremely high EA and a large band gap. In order to enhance hole injection into the emitting layer, 5% DPBIC was co-evaporated with 10% NHC blue emitter and 85% of an organic wide band gap host material based on moieties with high triplet energy such as carbazole or dibenzofurane to form the 40 nm emissive layer (EML). Note that the high glass transition temperature T_g of this host yields an organic glass providing a stable dispersion of emitters in the matrix. A 5 nm layer of the pure host was then evaporated as a hole blocking layer (HBL), followed by a 20 nm electron transport layer (ETL) containing another organic

electron transporter (ET) doped with lithum quinolate (LiQ) in even ratio, in order to ensure an Ohmic contact at the potassium/fluoride (KF) (6 nm)/Al (100 nm) cathode.

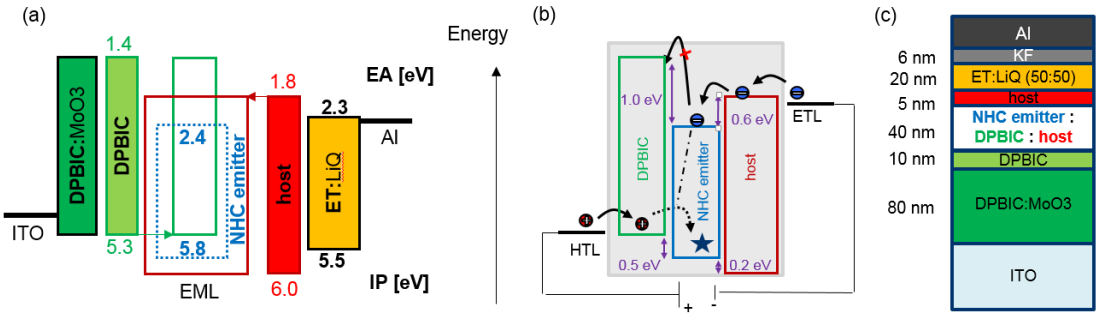

Figure 1(a) Energy level diagram of the blue PHOLED. Electron affinities (EA) as obtained from density functional theory and ionization potentials (IP) from UPS measurements; (b) scheme of energy levels and charge transport in the emitting layer which contains 5% DPBIC, 10% NHC emitter and 85% host: electrons are transported via the emitter and holes via DPBIC until a negatively charged emitter attracts a hole for charge recombination (dashed line); (c) schematic of PHOLED stack, see text for abbreviations.

5.3 Transient electroluminescence measurements

5.3.1 Principle

In order to investigate the charge transport in such a multi-layer structure with composite emissive layer we apply the transient electroluminescence (TEL) method to determine the transit times (τ) of the charge carriers in the device. Unlike the time-of-flight (TOF) method, which requires a thick (~µm) semiconductor film and blocking contacts, TEL can be applied to OLEDs with ~100 nm active layer thickness and Ohmic contacts. In TEL the delay between the application of a voltage pulse and the appearance of electroluminescence is measured. For this, a rectangular pulse voltage with certain amplitude is applied to the devices. After the voltage is switched

on, both injected electrons and holes will start moving driven by the electric field until they meet in the emissive layer and recombine to produce electroluminescence. As a result, there is a delay time τ between the voltage onset and light output. This delay time is correlated with the transit time of both charge carriers.

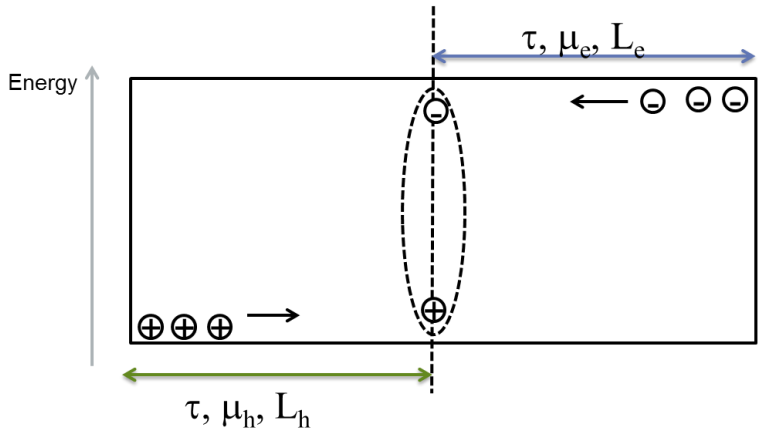

Figure 2. Schematic charge transport and recombination in transient electroluminescence measurement.

Figure 2 schematically shows in one dimension the charge transport and recombination process through a semiconductor layer with thickness L. After injection, the electrons and holes will recombine after a certain time τ. The distance travelled by electrons and holes is given by $L_e = E \times m_e \times t$ and $L_h = E \times m_h \times t$, respectively, with E the applied electric field, μ_e the electron mobility and μ_h the hole mobility. The delay time τ between voltage and light output is then given by $t = L / (E \times (m_e + m_h))$. It should be noted that the travelling time of electrons and holes is equal, but the distance they each travel depends on their respective mobilities. In case that $m_e << m_h$, holes will travel most of the distance of L and recombine with the slow electrons close to the electron injecting contact. As a result, the delay time approaches the hole transit time τ_h, given by $t_h = L / (E \times m_h)$. From the measured delay time the hole mobility can then be calculated. Vice versa, when $m_e >> m_h$, recombination will take place at the hole injecting anode, and the delay time τ will represent the transit time of electrons τ_e.

As a result, for unbalanced transport the measured delay time can be correlated to the transit time of the *fastest* carrier. Furthermore, when the electron and hole mobilities are equal, both charge carriers will travel to the middle of semiconductor layer and recombine. In that case, t will be determined by the mobility of both carriers as $t = L / (E \times (m_e + m_h)) = L / (2E \times m_h)$, and will be half of the hole- or electron transit time.

Experimentally, an Agilent 8114A pulse generator was used to input a voltage pulse. The width of the pulse τ_{pulse} was increased from 2 µs to 800 µs, and the pulse amplitude was varied gradually from 3 V to 6 V with steps of 0.5 V. The period was set to be 1ms. The time-integrated light output (l_{out}) was measured by a Keithley 6514 electrometer in current mode. When $\tau_{pulse} >> \tau$, a linear relation between l_{out} and τ_{pulse} is obtained, the intercept of the linear part with the τ_{pulse}-axis is corresponding to the delay time τ. [1] The relative accuracy in the obtained delay time amounts to ± 2% of the measured value.

5.3.2 Operation of pristine device

As shown in Figure 1b the ionization potential of the hole transporter DPBIC is shallower than that of the blue emitter and of the host. As a result, for sufficiently high DPBIC concentration (≥5%) the holes in the emitting layer will be carried by DPBIC. Furthermore, as the electron affinity of the blue phosphorescent NHC emitter is deeper than that of DPBIC and the host, the electrons in the emitting layer are carried by the NHC emitters when their concentration is sufficiently high. To disentangle the contributions of electrons and holes on the measured transit time devices were fabricated with 10% NHC emitter and a varying concentration x% of DPBIC hole transport units (x= 5%, 7.5% and 10%), co-deposited with the host material to form the 40 nm emitting layer. The transit times of pristine devices were then measured by transient electroluminescence measurement. As an example a TEL measurement on a PHOLED with 7.5% DPBIC hole transporter in the emissive layer is shown in Figure 3. The light-output l_{out} as a function of the applied voltage pulse width (t_{pulse}) is plotted. The intercept of the linear part at long pulse widths with the t_{pulse}-axis

corresponds to the delay time between application of the voltage and appearance of the electroluminescence.

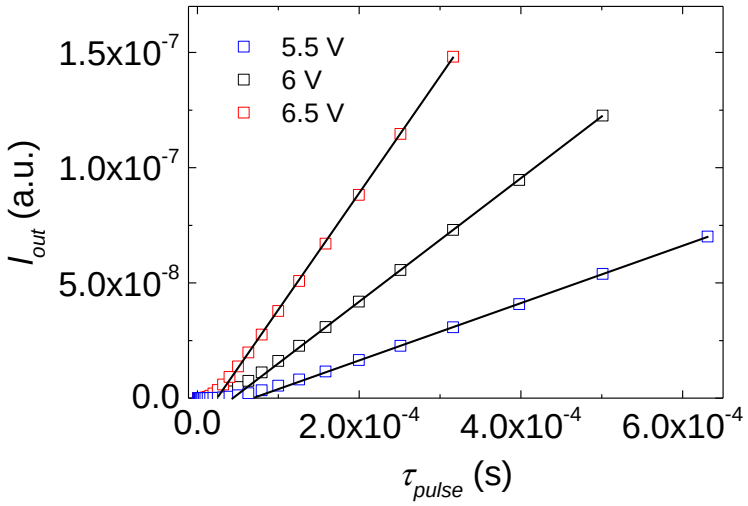

Figure 3. Transient electroluminescence measurements of pristine PHOLEDs containing 7.5% DPBIC and 10% NHC emitter in the EML. The symbols correspond to the measured integrated light-output for various applied voltages. The solid lines are linear fits to the data at long pulse width, their intercept with the τ_{pulse} -axis corresponds to the delay time τ.

In Figure 4 the measured delay times are plotted as a function of voltage for PHOLEDs with a varying concentration x% of DPBIC hole transport units with x=5%, 7.5% and 10%, respectively. We observe that the delay time is independent of the DPBIC concentration which demonstrates that the measured delay time corresponds to the transit time of the electrons in the PHOLED. For 10% NHC emitter concentration the electron transport is dominant over the hole transport, with x=5-10% of DPBIC hole transport units. This can be rationalized in terms of a higher (or equal) emitter concentration in combination with a smaller trapping depth for the electrons on the NHC emitter versus holes on DPBIC (compare EA and IP to those of the majority compound being the organic host in Figure 1 b). Consequently, the PHOLED current is dominated by the electron transport, not by holes, which we will also

confirm later by varying the emitter concentration (Figure 8).

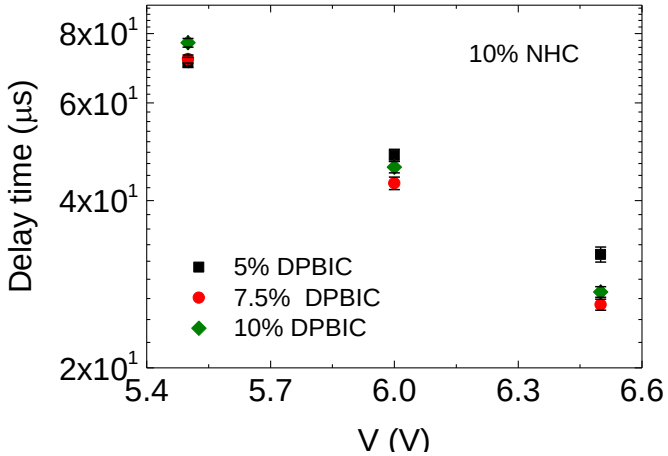

Figure 4. The delay time of pristine devices with *x*=5%, 7.5% and 10% DPBIC hole transporter and 10% NHC emitter in the emitting layer, respectively.

To further investigate the effect of DPBIC hole transport units on the charge transport also PHOLEDs with a 40 nm EML with an increased amount of 20% electron transporting NHC emitter units and *x*% DPBIC (x=0%, 5%, 10% and 15%) were fabricated. For 20% emitter the electron transport is always dominant and the measured delay times will represent the electron transit times. The delay time was measured for the pristine devices with a voltage pulse of amplitude from 4.5V to 6V, as shown in Figure 5. We observe that with increasing DPBIC concentration the delay time approximately doubles. This increase of the electron transit time could on the one hand be due to improved hole injection with higher DPBIC concentration leading to lower turn-on voltages (meaning that the voltage axis in Figure 5 might be shifting especially between 0% and 5%). On the other hand, also enhanced energetic disorder on the emitter could lead to lower electron mobility. As will be shown elsewhere, calculations of the energetic disorder in amorphous emission layers (obtained from molecular dynamics simulations) using the Thole model[8] (taking into account electrostatic and polarization interactions for a localized charge with its surrounding)

indicate that the width of the Gaussian density of states σ on the emitter is enhanced by ~20meV when increasing the DPBIC concentration from 0% to 15%. This is due to the strong electrical dipole of DPBIC (8Debye as obtained from DFT calculations for a single molecule in the gas phase) compared to the unipolar host (1Debye). Such an increase of σ then easily leads to a decrease of the electron mobility of a factor of two, as shown by kinetic Monte-Carlo simulations for single electrons in these morphologies. The longer transit time at higher DPBIC concentration is then a result of the fact that the presence of DPBIC molecules slows down the electron transit time over the emitter molecules due to increased energetic disorder.

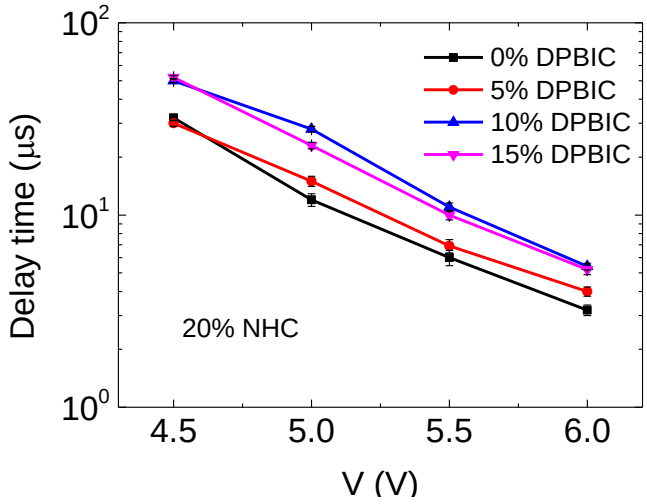

Figure 5. The delay time of pristine devices with x=0%, 5%, 10%, and 15% DPBIC hole transporter and 20% NHC emitter in the emitting layer, respectively.

5.3.3 Operation of degraded PHOLEDs

To investigate the degradation mechanism of our devices the change of charge transport and recombination process upon aging of the PHOLED will be investigated with transient electroluminescence. As the first step, the influence of DPBIC concentration on the stability of the PHOLEDs is tested. For this purpose, PHOLEDs with 40 nm EML containing 10% NHC emitter and x% DPBIC (x=5%, 7.5% and 10%) hole transporter were electrically aged. For device degradation, PHOLEDs were aged for different periods (from 10 min to 5 days) by applying a constant current density of

25 mA/cm^2, corresponding to a high initial luminance of L_0=6700 cd/m^2. Subsequently, transient electroluminescence measurements were carried out on pristine and aged pixels. As shown in Figure 6a for a voltage pulse amplitude of 6V pixels aged for longer periods show longer delay times. However, comparing the delay times for different DPBIC concentrations in the EML demonstrates that all pixels exhibit a similar trend of delay time increase with device aging time, independent of DPBIC concentration, especially for the first 25h where the LT70 has been reached. A linear increase of the delay time τ as a function of aging time, corresponding to a mobility decrease of $\mu_e \sim 1/t$, is clearly visible across the whole aging period. Furthermore, also the decay of the (normalized) electroluminescence shows only a weak dependence on the DPBIC concentration (Figure 6b), showing that the amount of DPBIC hole transport dopant in the range of x=5%-10% has no significant effect on the degradation process of the PHOLEDs. This is in agreement with the earlier observation on pristine PHOLEDs and shows that electrons are the dominant carriers, also in degraded samples.

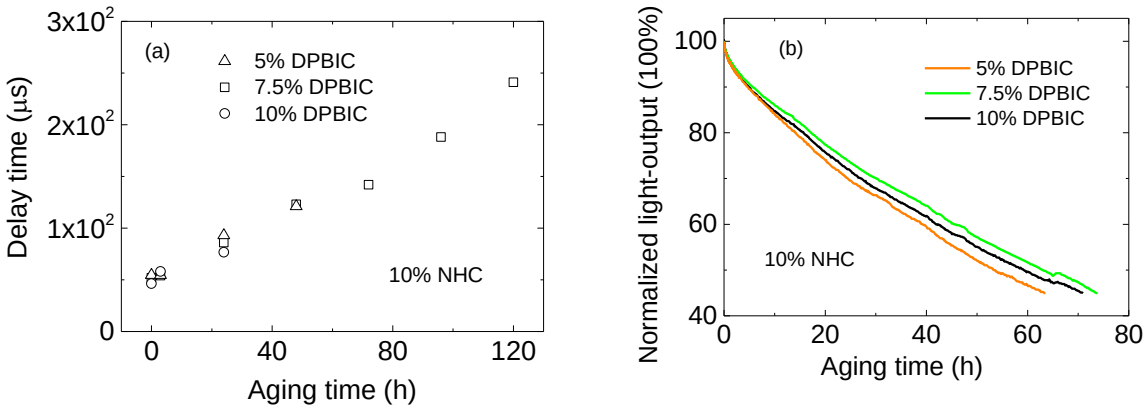

Figure 6. (a) Evolution of delay time during electrical aging of PHOLEDs and (b) normalized luminance-time curve stressed under J=25 mA/cm^2 (L_0=5500 cd/m^2) for devices with x% DPBIC and 10% NHC emitter in the EML; x=5%, 7.5% and 10%, respectively.

For the pixels that were aged for different time periods the J-V characteristics and efficiencies were also recorded, as shown in Figure 7a for a PHOLED containing 7.5%

DPBIC and 10% NHC emitter. During degradation the current decreases gradually with aging time, with the decrease more pronounced in the low voltage regime. A similar trend was observed for the efficiency, as also appears from Figure 6b. Figure 7b depicts the evolution of the delay time of PHOLEDs containing 7.5% DPBIC and 10% NHC emitter in the EML upon aging. For each pulse amplitude (5.5 V to 6.5 V), the delay time increases with aging time, in line with the decrease of the PHOLED current. It appears that when the PHOLED current at 6V decreases one order of magnitude after 5 days of aging, the measured delay time increases about 5 times, implying that the delay time increase is strongly correlated to the PHOLED current decrease during aging. Since the measured delay time represents the electron transport, the observed increase indicates that the electron transport is degraded upon aging. This rules out degradation within the EBL where only the hole mobility is relevant. Since the electron mobility within the ETL and HBL is much higher than in the emissive layer (due to trapping on the emitter) we can also rule out degradation in those layers as the delay time increases linearly already for short aging time in Figure 7b.

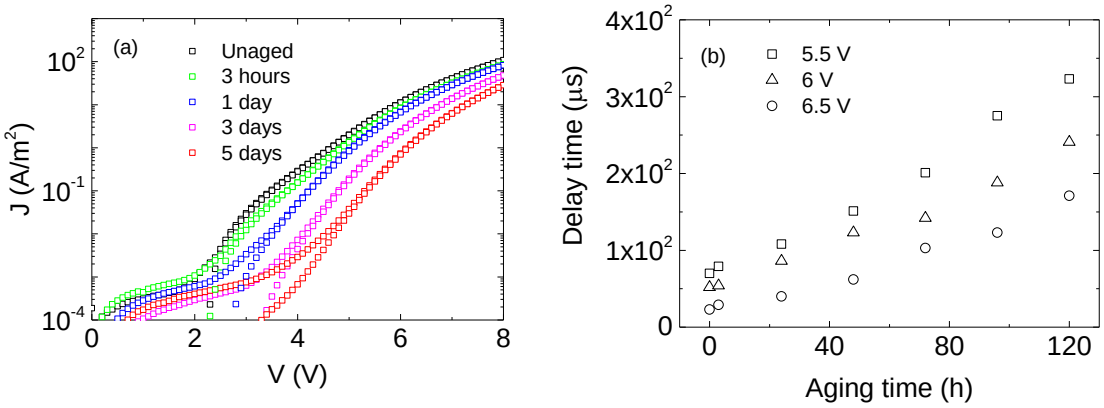

Figure 7. (a) *J-V* characteristics of PHOLEDs with 7.5% DPBIC and 10% NHC emitter as function of aging time at J=25 mA/cm2 and (b) evolution of delay time during aging of these devices for varying applied voltage.

In pristine PHOLEDs the transport is dominated by electrons that are carried by the

NHC emitters. For a decrease of the electron transport there are two possibilities: either the emitter molecules degrade and form inert complexes that do not participate in the transport or recombination anymore. In that case the reduction of the electron transport and mobility simply results from a decrease in the number of active transport sites. The other possibility is that degraded emitters or other degradation products e.g. form DPBIC or host act as electron traps, which even might act as luminescence quenchers. Then the decrease of the electron transport is a combined effect of reduced transport sites (if the emitter degrades) and additional electron trapping. In order to distinguish between those two mechanisms, PHOLEDs with emitter concentrations varying from 5% to 20% in the EML were fabricated, in combination with 10% DPBIC hole transport units. We observe for the pristine PHOLEDs that when the emitter concentration is decreased from 20% to 5% the electron transit time only increases by typically a factor of two as depicted in Figure 8, which can be explained by the slower electron mobility in case of lower emitter concentration. However, upon aging we observe that the electron transit times decreases 5 times. So if emitters would react to become only an electrically inactive species practically all of them would have to be converted in order to explain a five-fold increase of the transit time during degradation. With that, the efficiency of the PHOLED would be much lower as what is experimentally observed. Therefore, the reduction of the electron transport and increase of the delay time is most likely due to the creation of electron traps. However also the external quantum efficiency (EQE) of the OLEDs deteriorates during aging e.g in case of 10% emitter and 7% DPBIC the EQE drops by half from pristine to 60h aged samples at constant J=25 mA/cm^2 (Figure 6b). Therefore one has to further assume that the degradation products not only act as electron traps but also as luminescence quenchers. Finally, if one assumes that excitons are involved in the degradation process, it is most likely that this occurs close to the interface to the hole injecting DPBIC layer where recombination takes place during the whole aging process as the devices always remain electron dominated.

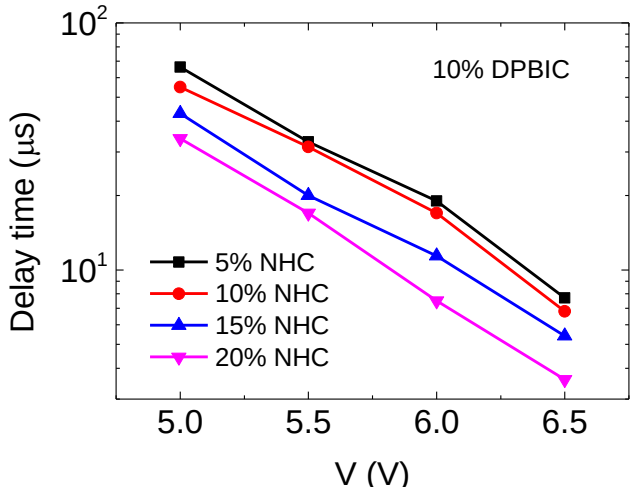

Figure 8. The delay time of pristine PHOLEDs with 10% DPBIC and *x*% NHC emitter in the 40 nm EML, with *x*=5%, 10%, 15% and 20% respectively.

5.4 Conclusion

In conclusion, the charge transport in blue PHOLEDs based on cyclometallated N-heterocyclic carbene (NHC) iridium complexes as emitters was investigated by transient electroluminescence. In these PHOLEDs the holes in the emissive layer are carried by DPBIC hole transport units, whereas the electrons are transported by the NHC emitter. Transient electroluminescence measurements show that for 10% of NHC emitter and 10% DPBIC co-evaporated in an organic host matrix the transport is dominated by electrons. Furthermore, varying the amount of DPBIC hole transport units between 5% and 10% has no effect on the degradation process of the PHOLED showing that the devices remain electron dominated also during aging. The decrease of the PHOLED current in aged devices is correlated with the increase of the electron transit time. The degraded electron transport and efficiency can be explained by the creation of electron traps that also act as luminous quenchers during aging.

References

[1] P. W. M. Blom, M. C. J. M. Vissenberg. *Physical Review Letters* **1998**, *80*, 3819.

[2] V. Sivasubramaniam, F. Brodkorb, S. Hanning, H. Loebl, V. Elsbergen, H. Boerner, U. Scherf, M. Kreyenschmidt. *Open Chemistry* **2009**, *7*, 836.

[3] V. Sivasubramaniam, F. Brodkorb, S. Hanning, H. P. Loebl, V. van Elsbergen, H. Boerner, U. Scherf, M. Kreyenschmidt. *Journal of Fluorine Chemistry* **2009**, *130*, 640.

[4] R. Seifert, I. Rabelo de Moraes, S. Scholz, M. C. Gather, B. Lüssem, K. Leo. *Organic Electronics* **2013**, *14*, 115.

[5] A. D. Becke. *Physical review A* **1988**, *38*, 3098.

[6] J. P. Perdew. *Physical Review B* **1986**, *33*, 8822.

[7] T. B. Tai, S. U. Lee, M. T. Nguyen. *Physical Chemistry Chemical Physics* **2016**, *18*, 11620.

[8] A. Klamt, G. Schüürmann. *Journal of the Chemical Society, Perkin Transactions 2* **1993**, 799.

[9] P. Erk, M. Bold, M. Egen, E. Fuchs, T. Geßner, K. Kahle, C. Lennartz, O. Molt, S. Nord, H. Reichelt, C. Schildknecht, H.-H. Johannes, W. Kowalsky. *SID Symposium Digest of Technical Papers* **2006**, *37*, 131.

Summary

After 30 years development, organic light emitting diodes have been widely used in recent displays industry and are believed to be the most promising candidate for the next generation of planer and flexible lighting. However, the most critical issue around this technology is the device lifetime and the mechanisms behind device efficiency loss under long-term operation. Although investigated intensively in the past, the complexity of device architectures and materials made the understanding of OLED degradation mechanisms quite difficult. Possible mechanisms such as chemical reactions, formation of traps, accumulation of charges, increase of injection barriers, and decrease of carrier mobilities have been suggested in previous reports.

In this thesis, to simply the problem, in Chapter 2 and 3 we have investigated the degradation of polymer LEDs with a simple single layer structure. Another big advantage is that our understanding on PLED operation has been well developed in the past decades. For instance, it has been found the hole transport in PLEDs is space charge limited with a trap-free characteristic with the hole mobility depends on the electric field, the charge density and the temperature. On the other hand, the electron transport is strongly limited by charge trapping. Furthermore, trapped electrons can capture the free holes via non-radiative trap-assisted recombination which competes with the radiative Langevin recombination of free holes with free electrons and thereby play a role of main loss process for the device efficiency. Presently, the *JV* characteristics and device efficiency of PLEDs can be numerically predicted when the hole mobility and the trap parameters for electrons are known. This numerical model has been used in Chapter 2 to distinguish possible mechanisms for PLED degradation. By individually changing the device parameters, it has been found an increase of injection barriers, a decrease of mobility and increase of electron traps cannot explain the observed experimental phenomena during device aging. The strong decrease of PLED current, which even gets lower than the pristine hole current implies the

degradation of hole transport during this process. From numerical simulation, the generation of hole traps simultaneously explained the decrease of *JV* characteristic and efficiency of degraded PLEDs. The formation of hole traps also induces a shift of the recombination profile towards the anode. Transient electroluminescent measurement further confirms the degradation of hole transport.

Subsequently, in Chapter 3 by evaluation of the voltage drift of a PLED upon aging, the density of hole traps as function of aging time has been calculated. With the amount of hole traps known, the luminance decay of the PLED could be predicted. The agreement with experiment demonstrates that the decrease of the radiative recombination under stress is a direct consequence of increased non-radiative recombination of trapped holes with free electrons. It has been found that initially the density of hole traps increases linearly with time, and after a short stress period the trap formation is slowed down to a square root dependence on time. The observed hole trap generation could be linked to the product of exciton density and density of free holes. Hole trap formation due to the interaction between triplet excitons and free holes (polarons) enables unification of the degradation of various PPV derivatives.

The information of hole trap generation during PLED aging has then been used to understand the negative contribution to the capacitance observed in the low frequency *C-V* characteristics of bipolar PLEDs in Chapter 4. It has been found the negative contribution is characterized by a voltage independent relaxation time that is in the same order of magnitude as the inverse rate for trap-assisted recombination. Enhancement of the amount of electron traps by the addition of fullerene molecules leads to a more pronounced NC effect, which can be quantitatively explained by trap-assisted recombination. Furthermore, the enhanced NC effect in degraded PLEDs, in which hole traps are generated by current stress, can be attributed to trap-assisted recombination of free electrons with trapped holes. The absence of NC in a nearly trap-free PLED unambiguously shows that trap-assisted recombination is the only mechanism responsible for the negative contribution to the capacitance in bipolar

organic diodes.

In Chapter 5 transient electroluminescence measurement has been applied to investigate the charge transport and the degradation of phosphorescent blue OLED with multi-layer structure and double-host mixed with guest (cyclometallated N-heterocyclic carbene iridium complexes) emitting system. In the emissive layer of the OLED, holes are carried by DPBIC hole transport units, whereas the electrons are transported by the guest emitter. The measurements show that for 10% of emitter and 10% DPBIC co-evaporated in an organic host matrix the transport is dominated by electrons. Varying the amount of DPBIC hole transport units between 5% and 10% has no effect on the degradation process of the OLED showing the devices remain electron dominated also during aging. The decrease of the OLED current in aged devices is correlated with the increase of the electron transit time. The degraded electron transport and device efficiency can then be explained by the creation of electron traps which act also as luminous quenchers during device aging.

Publications

- **Q. Niu**, G. J. A. Wetzelaer, P. W. Blom, N. I. Crăciun. Modeling of Electrical Characteristics of Degraded Polymer Light-Emitting Diodes. *Advanced Electronic Materials* **2016**, 2(8), 1600103
- **Q. Niu**, G. J. A. Wetzelaer, P. W. Blom, N. I. Crăciun. Degradation of polymer light-emitting diodes by hole trap formation. *In preparation*.
- **Q. Niu**, P. W. M. Blom, F. May, P. Heimel, M. Zhang, C. Eickhoff, U. Heinemeyer, C. Lennartz and N. I. Crăciun. Transient electroluminescence on pristine and degraded phosphorescent blue OLEDs. *Submitted.*
- **Q. Niu**, P. W. Blom, N. I. Crăciun. Mechanism of negative capacitance in polymer light-emitting diodes. *In preparation.*
- I. Rörich, **Q. Niu**, P. W. Blom, N. I. Crăciun. Influence of electrical degradation on exciton lifetime in conjugated polymers. *In preparation.*